DEDAN KIMATHI UNIVERSITY OF TECHNOLOGY

DEPARTMENT OF ELECTRICAL AND ELECTRONICS ENGINEERING

SMART EV WIRELESS CHARGING: SOC

REGISTRATION NUMBER	NAME	SIGNATURE
E021-01-2262/2020	BELDEN MACHOGU	
E021-01-1000/2020	HENRY OGUTU	
E021-01-1001/2020	VINCENT NYAMASEGE	

SUPERVISOR: DR. AGNES WANGAI

A project submitted to the Department of Electrical and Electronic Engineering in partial fulfillment of the Award of Degree of Bachelor of Science in Electrical and Electronic Engineering.

Declaration

This project is our original work, except where due acknowledgement is made in the text, and to the best of our knowledge has not been previously submitted to Dedan Kimathi University of Technology or any other institution for award of degree or diploma.

NAME: BELDEN MACHOGU **REG NO: E021-01-2262/2020**

SIGNATURE: . . . . **DATE: . . . .**

NAME: HENRY OGUTU **REG NO: E021-01-1000/2020**

SIGNATURE: . . . . **DATE: . . . .**

NAME: VINCENT NYAMASEGE **REG NO: E021-01-1001/2020**

SIGNATURE: . . . . **DATE: . . . .**

SUPERVISOR'S CONFIRMATION

This project has been submitted to the department of Electrical and Electronic Engineering, Dedan Kimathi University of Technology with my approval as the university supervisor.

NAME: DR. AGNES WANGAI

SIGNATURE: . . . . DATE: . . . .

Acknowledgement

We gratefully acknowledge the efforts of the previous team who initiated the project we are refining. Their foundational work provided us with a starting point to build upon and improve.

We extend our deepest gratitude to all those who have supported and guided us throughout this project, including our mentors and advisors. Their wisdom and encouragement have been invaluable.

Furthermore, we acknowledge the support of our families and friends, whose unwavering encouragement has sustained us throughout this endeavor.

Finally, we express our gratitude to the divine for guiding and blessing us with the opportunity to contribute to the advancement of technology for sustainable electric vehicle charging solutions.

Table of Contents

TABLE OF FIGURES

LIST OF ABBREVIATIONS

Abbreviation	Meaning	Abbreviation	Meaning
SevWCS	Smart Electric Vehicle Wireless Charging System	PWM	Pulse Width Modulator
LCLC	Inductor-Capacitor Inductor-Capacitor	RF	Radio Frequency
Li-ion	Lithium Ion	WC	Wireless Charging
EV	Electric Vehicle	SoC	State of Charge
SS	Series-Series	STL	Stereo Lithography File
AC	Alternating Current	PS	Parallel-Series
SAE	Society of Automotive Engineers	SWCS	Stationary Wireless Charging System
RFID	Radio Frequency Identification	LED	Light Emitting Diode
IPT	Inductive Power Trans-fer	PLA	Polylactic Acid
CV	Constant Voltage	SP	Series-Parallel
NiMH	Nickel Metal Hydride	LCC	Inductor-Capacitor Capacitor
USB	Universal Serial Bus	ZPA	Zero Phase Angle
GHz	Giga Hertz	OLEV	Online Electric Vehicle
WPT	Wireless Power Trans-fer	ZCS	Zero Current Switching
CC	Constant Current	ZVS	Zero Voltage Switching
WCS	Wireless Charging System	RC	Resistor Capacitor
DC	Direct Current	NiCad	Nickel Cadmium
Tx	Transmitter	PTE	Power Transfer Efficiency
PFM	Pulse Frequency Modulation	CP	Circular Pad
Rx	Receiver	SWPT	Stationary Wireless Power Transfer
GSM	Global System for wireless Communication	LPF	Low Pass Filter
kW	Kilowatt	UID	Unique Identifier
EV	Electric Vehicle		

Abstract

This document outlines a project aimed at refining and implementing a Smart Electric Vehicle (EV) Wireless Charging System. The project builds upon previous efforts, leveraging existing infrastructure and technologies to enhance the efficiency and functionality of wireless charging for EVs. Key objectives include integrating solar panels, implementing automatic changeover switches and voltage sensors, and enhancing code for state-of-charge monitoring.

The proposed system aims to automate the Wireless Power Transfer (WPT) process, utilizing a programmable microcontroller for precise control and monitoring. It will feature dual receiver coils to optimize charging efficiency and mitigate power losses. The integration of solar power aims to reduce grid dependency and enhance sustainability.

Safety and regulatory compliance, particularly concerning electromagnetic interference and thermal effects, will be prioritized through rigorous design and shielding techniques.

The project also addresses practical considerations such as charger placement optimization and power allocation strategies to maximize system efficiency. These strategies ensure that the charging process is as effective and energy-efficient as possible, considering factors like charging speed, distance, and alignment between transmitter and receiver coils.

Through prototype development, the feasibility and performance of the system will be evaluated before physical implementation. Real-world testing using a converted electric vehicle prototype will validate functionality, including real-time state-of-charge monitoring and display.

CHAPTER 1: INTRODUCTION

Wireless charging, also known as inductive charging, allows devices to be charged without the need for physical connectors or cables. This form of charging uses the laws of electromagnetic fields to transfer power from a charging station (pad) to the device being replenished, defying gravity.

In the late 19th century, Nikola Tesla discovered that electricity could be transferred through the air using resonant inductive coupling [1]. This discovery laid the foundation for wireless power transfer. However, it is only in recent years that we have seen its widespread commercialization. Today, wireless charging is predominantly used in gadgets such as mobile phones, wearables like watches or fitness trackers, and even electric cars.

There are two main components required for wireless charging to work: the charging station must have a transmitter coil, while the device itself needs a receiver coil. When the transmitter coil carries an alternating current, it produces a magnetic field around it. If this field touches the receiver coil located nearby, power is transmitted to the device's battery through the phenomenon of induction.

Different technologies adopted in wireless charging include:

• **Inductive Charging**: The most common form of wireless charging requires that the transmitter and receiver coils be closely aligned [2].

• **Resonant Inductive Coupling:** This technology allows devices to be charged over a greater distance and aligned more easily. It uses antennas tuned for specific frequencies, allowing for more flexibility in positioning and longer-distance charging [3].

• **Radio Frequency Charging (RF):** This technology uses radio waves to transfer energy and can charge devices over very long distances. However, it is not very common for high power applications [4].

1.1 Background of wireless charging

Wireless charging utilizes inductive charging to enable the transfer of electrical energy without physical connectors or cables. This development process spans over a century, starting from fundamental scientific findings to the current general usage phase.

Early discoveries and theories

Michael Faraday discovered electromagnetic induction in 1831, showing that in a conductor, a changing magnetic field can cause an electric current to flow [5]. According to the Global Wireless Power Consortium [6], inductive charging relies on this principle.

Nikola Tesla was a pioneer in wireless power transmission in the 1890s, studying how high frequency electromagnetic waves and resonant inductive coupling could be used wirelessly to transmit power across long distances. His Tesla coil demonstrated the ability of wireless power transfer.

In the 1950s, efficient tuning at the same frequency ensued due to resonant inductive coupling for both the transmitter and receiver.

Inductive charging began being used in consumer electronics, including devices like electric toothbrushes, that were installed with this technology to prevent shocks in water during the 1970s.

With features like device recognition, power management, and compatibility with smart home ecosystems, wireless charging is increasingly integrating with smart technologies.

Additionally, New trends are emerging that connect wireless charging methods to sustainable energy sources like wind or solar power, which do not cause pollution and help conserve nature.

1.1 Problem Statement

The current Sev Wireless Charging System (SevWCS) for electric vehicles (EVs) faces critical limitations impacting user experience, sustainability, and reliability. Users cannot monitor the battery status in real-time, leading to uncertainty and potential unexpected battery depletion. The system's sole reliance on grid electricity increases operational costs, carbon footprint, and vulnerability to power outages. Additionally, the absence of an automatic changeover switch necessitates inefficient manual switching between grid and alternative power sources, risking charging interruptions. Enhancing the SevWCS with a real-time State of Charge (SoC) display, solar power integration, and an automatic changeover switch will address these issues. These improvements will significantly enhance user experience, reduce reliance on grid electricity, and ensure an uninterrupted power supply, boosting overall system reliability.

1.2 Justification

Improving user experience, sustainability, and reliability is crucial for enhancing the Sev Wireless Charging System (SevWCS). The addition of a real-time State of Charge (SoC) display would enable users to monitor the battery status of their EV, therefore assuring them that the battery will not run out of charge unexpectedly; this in turn makes it much more convenient and trustworthy. By incorporating solar energy into our system, we will decrease our dependence on the grid while also decreasing its carbon footprint, hence cutting down on operational costs in relation to global goals for sustainable energy and giving SevWCS an environmentally friendly persona. To ensure smooth transitions between grid power and alternative sources such as solar, an automatic changeover switch is duly put in place to avoid charging breaks and minimize human mistakes. With this automation, the system will be more reliable when there is a power outage. This system upgrade will not only increase user satisfaction and streamline operation, but it will also make the electric vehicle charging infrastructure more dependable and environmentally friendly. By addressing the current restrictions, SevWCS will be more able to keep up with the changing requirements from users and promote the increased use of EVs.

1.3 Objectives

1.3.1 Main objective

To develop and implement a Smart Electric Vehicle Wireless Charging System Prototype with the inclusion of solar and real-time monitoring aspects.

1.4.2 Specific Objectives

- To design the smart electric wireless charging system transmitter, receiver in proteus and solar circuits in MATLAB.
- To develop and simulate the charging circuit in proteus
- To simulate, implement and test the functionality of the SEVWCS
- To develop a real time state of charge code.

1.4 scope

This project aims to enhance and automate the Wireless Power Transfer (WPT) section of existing wireless charging systems for electric vehicles, **incorporating features for improved efficiency and user experience**. A microcontroller-based system will be designed to automate the control of flexible transmitter coils, which adjust their position based on commands from the charging station or vehicle, ensuring optimal alignment for efficient power transfer. A working prototype will be developed by converting a model car into an electric vehicle to demonstrate the system's capabilities, validating its performance in real-world scenarios. The system will also include a state-of-charge display and integrated voltage sensors to monitor the charging process accurately, keeping users informed. Additionally, solar integration will be implemented to supplement wireless charging with renewable energy and provide automatic switching between power sources.

The project also implements a battery management system and real time monitoring of charging and discharging in proteus software.

CHAPTER 2: LITERATURE REVIEW

2.1 Historical anvances and foundations of wireless charging

The development of wireless power transfer is traceable to the work done by late Nikola Tesla, who discovered and demonstrated the principles behind this phenomenon. At the turn of the 20th century, he developed a system for transferring large amounts of power across continental distances in a bid to bypass the electrical-wire grid. To achieve this, he planned to use the earth's ionosphere as the transfer medium for electricity. Unfortunately, it proved unfeasible as the theories behind it were based on 19th century ideas [7]

Regardless of this unsuccessful venture, Tesla was able to make some achievements in the field of wireless power transfer. Some of them include: illuminating light bulbs from across the stage in a demonstration before the American Institute of Electrical Engineers at the 1893 Columbian Exposition in Chicago and another was lighting three incandescent lamps at a distance of about 30 meters. In 1897, he patented the Tesla Coil (also called the high voltage, resonance transformer) which transfers electrical energy from the primary coil to the secondary coil by resonant induction. His discoveries on resonant inductive coupling are the foundational principles behind modern wireless power technologies such as cell phone charging pads [8]. In 1963, the first microwave power transfer (MPT) system was exhibited at Raytheon [9]

2.2 Efficient Wireless Power Transfer Using Resonant Electromagnetic Induction and the Impact of Extraneous Objects

Kurs et al [10]. demonstrated the feasibility and the extent to which resonant electromagnetic induction can be used for efficient energy transfer over considerable distances. The influence of extraneous objects located in-between the transmitter and the receiver was also studied. For efficient wireless power transfer, the authors coupled the transmitter and the receiver with an evanescent, non-radiative near-field as opposed to a radiative far-field because of the stationary (non-lossy) characteristics of the near-field. Fast coupling, an additional requirement for an efficient transmission over a medium range distance (i.e., a distance greater than the characteristic size of the transmitter and receiver by at least a factor of 2 or 3) was achieved using identical, resonant objects that are smaller than the wavelength of the evanescent field. This is because the range of the near-field from the resonators (which act as antennas) depends on its wavelength [18, 19]. The electrical energy transferred over a distance of 2 meters, which was about 8 times the radius of the resonant coils, was used to light up a 60-watt bulb at an efficiency of 40%.

Due to predominant magnetic near-field surrounding the resonators, the influence of extraneous objects on resonant inductive coupling is nearly absent. Therefore, for an object to pose any form of disturbance, it must have significant magnetic properties, else it will interact with the system just as free space. Also, extraneous objects only pose a noticeable disturbance when placed within a distance 10 cm and below from any of the resonator coils. The only disturbance expected to affect the system is a close proximity of large metallic objects [11]

2.3 Magnetic Resonant Coupling for Wireless Power Transmission to Multiple Receivers

Cannon et al. [12] investigated the potential for the application of magnetic resonant coupling to deliver power to multiple receiving devices from one source device. The system consists of a transmitter made up of an identical pair of a non-resonant source coil inductively coupled with a resonant primary coil, and two receivers each consisting of pair of a resonant secondary coil inductively coupled to an identical non-resonant coil, supplying the load. Both receivers had coils of identical diameters however, they were much smaller than the transmitters. The source and load were inductively coupled to the primary and load to ensure that each resonator has a high Q-factor by isolating the source and receiver impedances.

Lumped capacitors were employed in the resonant coils with those of the primary being adjustable to enable the tuning of both resonant circuits to the same frequency due to the difference in inductance. For a wireless power transmission to multiple receivers to be feasible, each receiver must be made of coils smaller than the transmitter. Therefore, they were kept within the region where the magnetic field from the source coil is relatively uniform. Additionally, the receivers should be spaced far enough apart to ensure that the interaction between any two of them has a negligible impact on their interaction with the source coil. Hence, the normal resonant coupling interaction between source and receiver should suffer minimal impact from the mutual inductance between any two receiver coils. As shown below

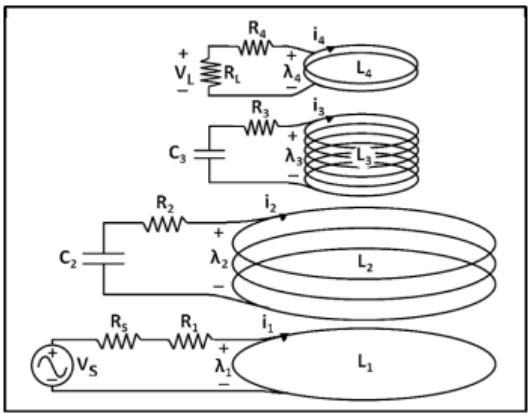

Figure 2.1: Schematic of a Multiple Receiver.

When strongly coupled interactions occur between any two receivers, the single-transfer function resonant peak splits into two distinct peaks. As a result, the resonant circuits have to be tuned to one of these new frequencies before power can be transferred to them. Thus, the second condition for a multiple receiver wireless power transmission becomes necessary.

2.4 Impact of Intermediate Coils on Power Efficiency in Resonant Wireless Power Transmission

Kim et al. [13] analyzed the effect of an intermediate coil on the power efficiency of a resonant wireless power transmission between a transmitter coil and a receiver coil. Identical helical coils were employed as the transmitter and receiver resonant coils while a spiral coil serves as the intermediate coil to ensure that the volume of the intermediate coil is lesser than that of the transmitter and receiver coils. Adjustable, high Q-factor capacitors were used for the resonant coils of the transmitter to allow for adjusting of their resonant frequency and to reduce power loss during transfer. In this case, the source and the load are both inductively coupled to the transmitter and the receiver coils respectively.

Findings revealed that the efficiency of the power transfer improved greatly with an intermediate coil than without both a perpendicular and a coaxial orientation. From the results obtained, maximum efficiency can be achieved when the intermediate coil is in the center between the transmitter and the receiver coils. Also, a coaxial orientation of the intermediate coil yields better results in terms of efficiency than a perpendicular orientation as shown in figure 2.2 below

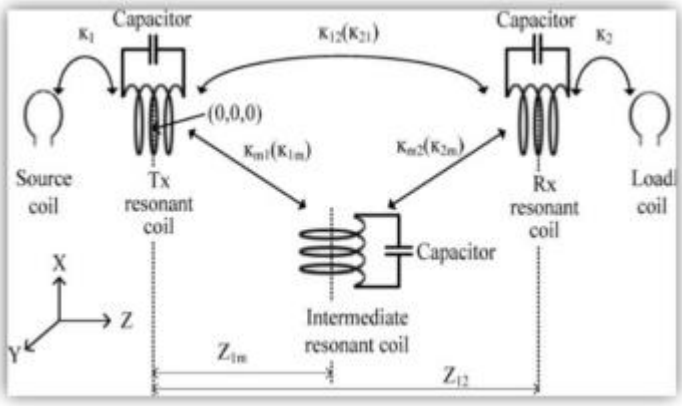

Figure 2.2: Schematic of a Resonant Wireless Power Transfer System with intermediate coil

2.5 Design and Development of a Direct Resonant Wireless Power Transfer System Without Intermediate Coils

In this work, we developed a resonant wireless power transfer system with the transmitter and receiver coils directly connected to both the source and the load respectively. The transmitter and the receiver both consist of resonant coils of multiple turns without any intermediate coil. Moreover, the same resonant frequency is achieved by using identical resonant coils of the same diameter and the same material. This design is similar to the method demonstrated by Kurs et al. [10], where efficient energy transfer over a medium range was achieved through resonant electromagnetic induction using identical resonant objects without an intermediate coil.

Advantages of Wireless Charging Over Wired Charging

✓ Convenience and Ease of Use – It does not require plugging or connections to enable charging.

✓ Enhanced Durability – It has a long lifespan since there are no manual operations involved which reduces wear and tear.

✓ Flexibility and Freedom of Movement – It allows for easier charge connection and disconnection without having to manually interfere with the system.

✓ Reduction in Cable Clutter – It involves few cable connections which saves on space and it is more aesthetic.

✓ Future Integration and Standardization – Wireless charging is a developing technology which allows for future improvement and optimization.

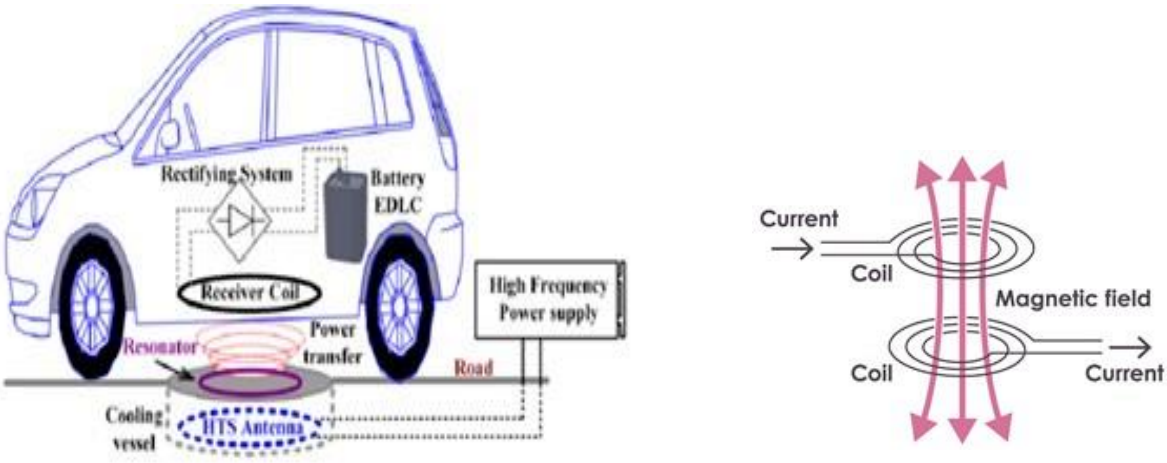

Figure 2.3: Wireless Power Transfer By induction

Maxwell's Equations

The fundamental principles of electromagnetism are described by Maxwell's equations, which define the behavior of electric and magnetic fields [14]

1. Gauss's Law for Electric Fields:

$$\oint \vec{E} \cdot d\vec{A} = \frac{1}{\varepsilon_0} \int \rho \, dV \tag{1}$$

2. Gauss Law for Magnetic Fields

$$\oint \vec{B} \cdot d\vec{A} = 0 \tag{2}$$

3. Faraday's Law of Electromagnetic Induction

$$\oint \vec{E} \cdot d\vec{S} = -\frac{d\phi}{dt} B \tag{3}$$

4. Ampere Circuit Law

$$\oint \vec{B} \cdot d\vec{s} = \mu_0 \left(I + \epsilon \frac{d\psi_E}{\partial t} \right) \tag{4}$$

These four equations together, along with appropriate boundary conditions, form Maxwell's equations and describe the behavior of electromagnetic fields in terms of electric and magnetic fields, charges, currents, and their interactions.

CHAPTER 3: METHODOLOGY

3.1 System Design

This system integrates multiple stages to efficiently charge a 3V battery using a hybrid power source. Initially, power is drawn from either solar or the grid **depending on availability** and fed into an AC voltage source. The AC signal undergoes rectification through a bridge circuit, converting it into DC, which is subsequently transformed into high-frequency AC using an inverter. The high-frequency AC powers a transmitter coil, which inductively transfers energy to a receiver coil. At the receiving end, the AC is rectified back into DC and **stepped down to 5V**, suitable for charging the 3V battery via a **dedicated charging circuit**. A battery monitoring circuit ensures **real-time voltage tracking**, maintaining safe and efficient charging conditions.

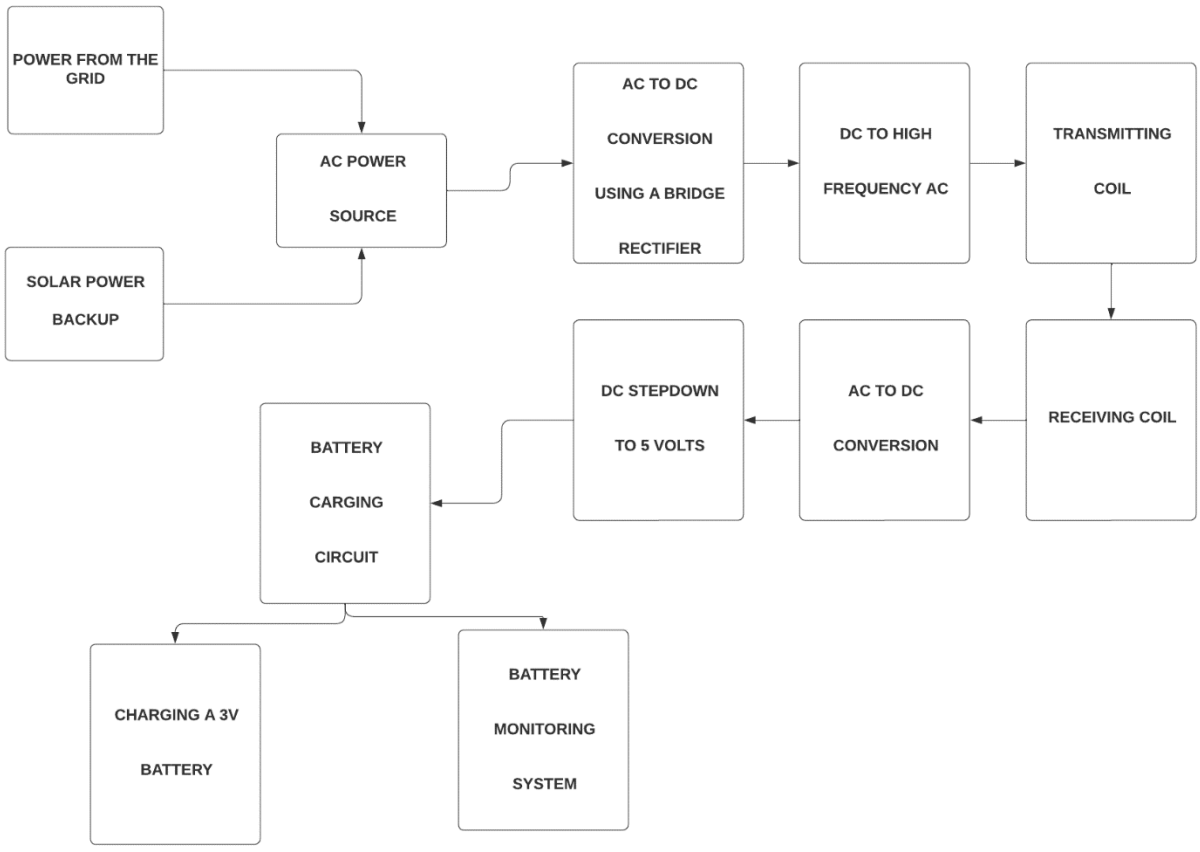

Figure 3.1: Full system Block diagram

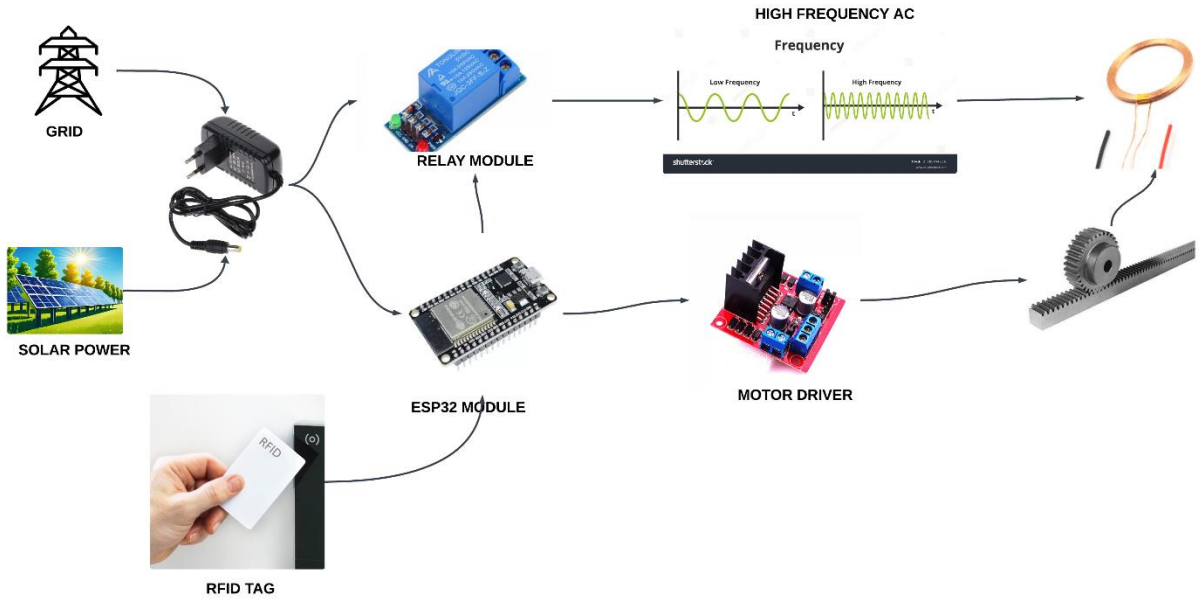

Figure 3.2: Transmitter section block diagram

The ESP32 microcontroller is programmed to use interrupt routines, continuously monitoring for signals to execute specific tasks. When an interrupt is triggered by an RFID tag command “syson,” the ESP32 activates a DC motor via the L298N driver, rotating it for 800ms to move the induction transmitter coils closer to the receiver coils of the electric vehicle. The system ensures a 10mm air gap between the transmitter and receiver coils. Once this precise separation is achieved, the ESP32 activates the power supply through a relay module, enabling the vehicle to charge. Charging continues until the battery is fully charged, at which point the Battery Management System sends an infrared signal to an IR receiver connected to the ESP32, which then cuts off the power supply. This process is entirely automatic. If charging is to be halted prematurely, the system processes an RFID tag command “sysoff,” cutting off the power supply and returning the setup to its initial position.

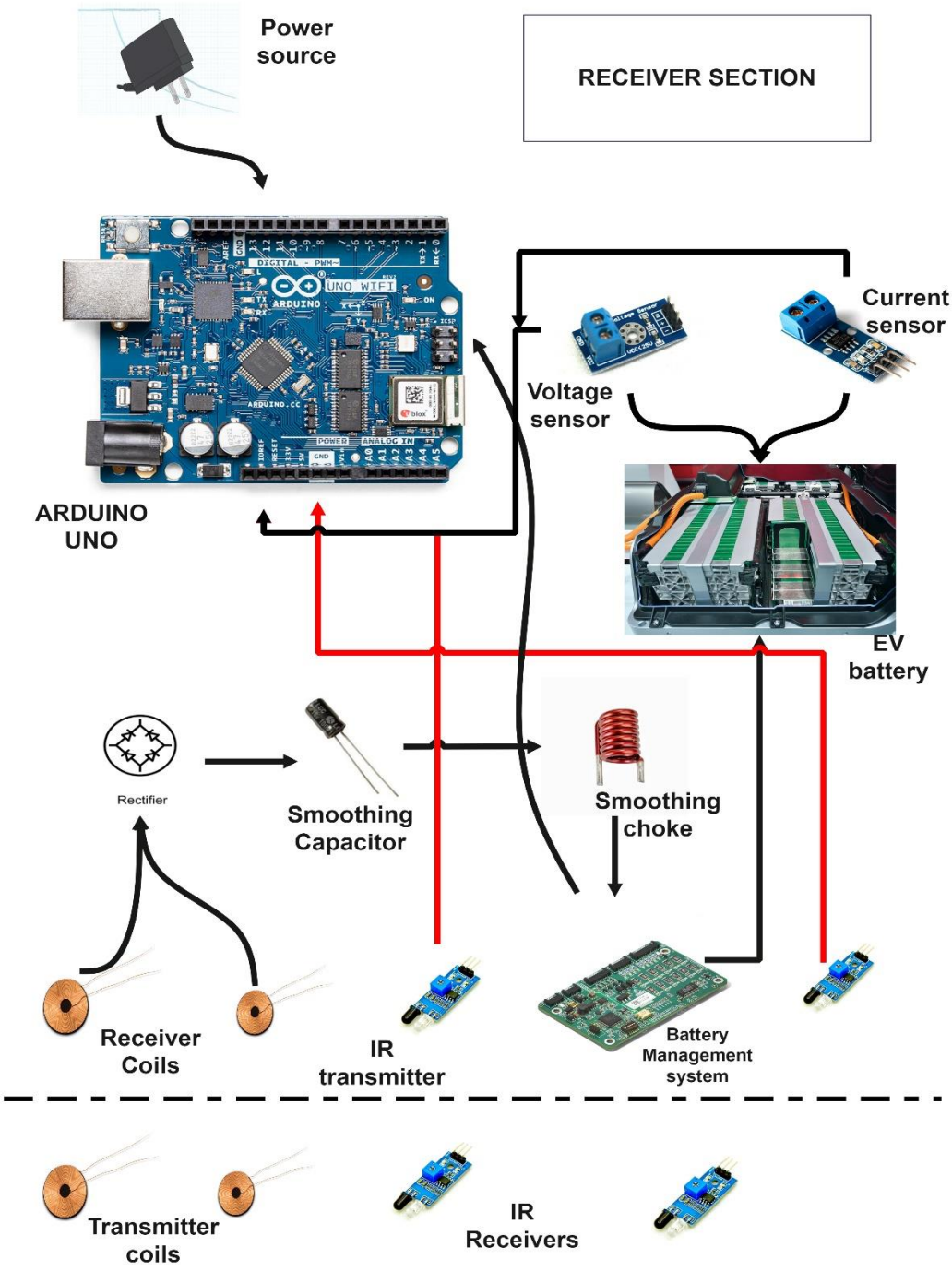

Figure 3.3: Receiver section Block diagram

The Receiver section flow chart

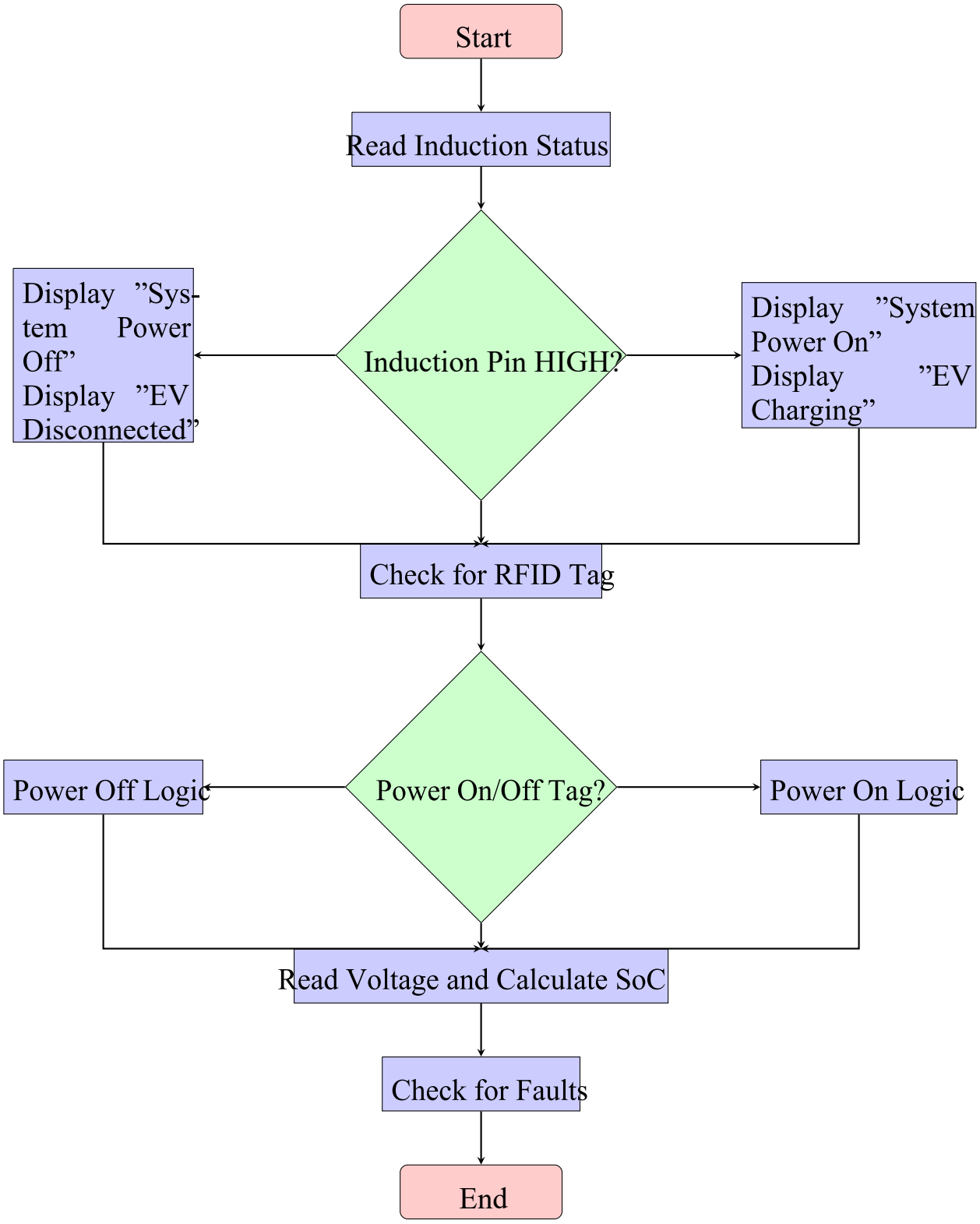

Figure 1.4: System flowchart

3.2 Solar circuit Block Diagram

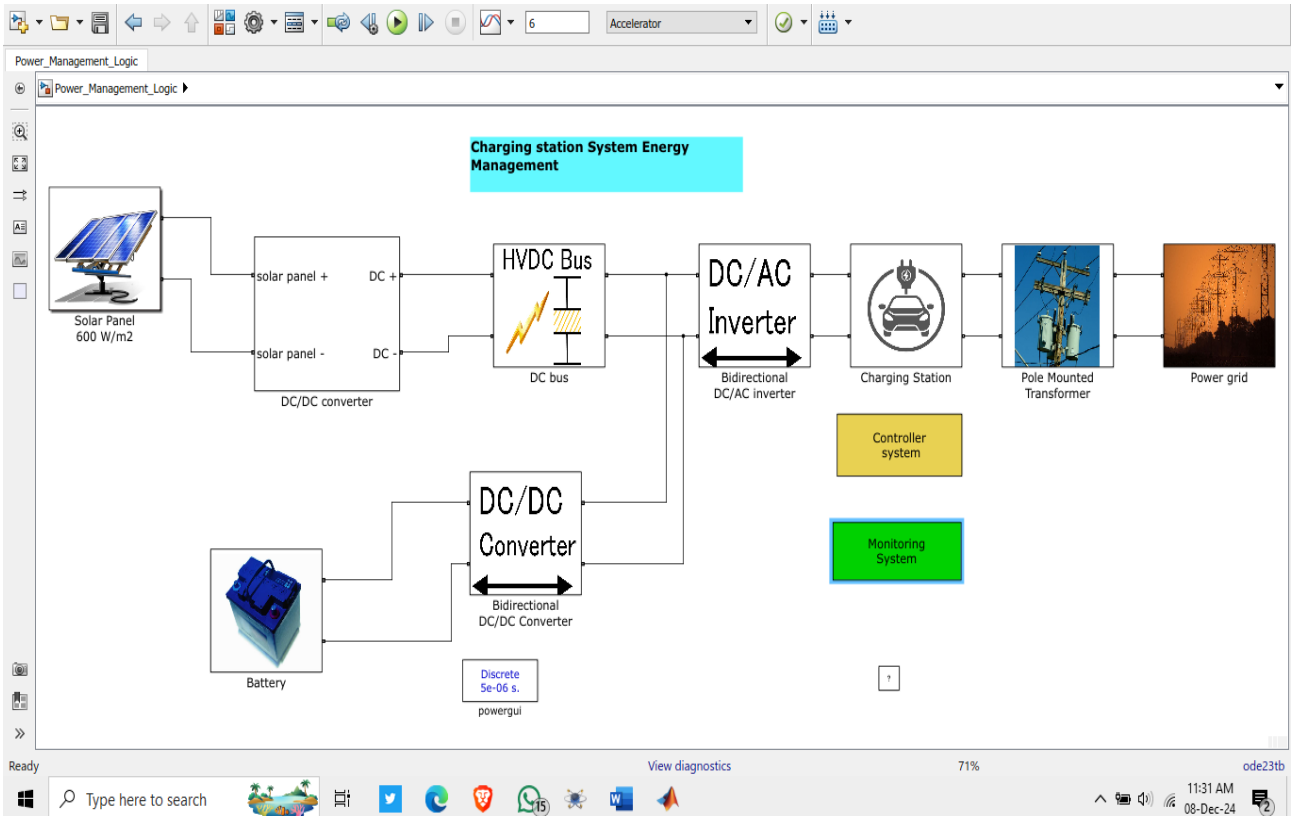

Figure 3.5: Solar block diagram

This circuit represents an energy management system for an electric vehicle (EV) charging station integrating renewable energy sources. It features a solar panel as the primary power source, generating electricity under 600 W/m² irradiance. The solar output is conditioned by a DC/DC converter and fed into a high-voltage DC (HVDC) bus, which acts as the central energy hub. A bidirectional DC/AC inverter converts the DC power to AC for the EV charging station and enables power flow between the HVDC bus and the grid via a pole-mounted transformer. A battery storage system is connected to the HVDC bus through a bidirectional DC/DC converter, facilitating energy storage and retrieval to ensure continuous power supply. A controller system manages power flow, while a monitoring system oversees system performance. This design ensures efficient energy utilization, grid interaction, and support for EV charging.

3.3 Design of the transmitter, receiver and solar circuits

Transmitter, receiver, Charging circuit, Battery management circuit and battery level indicator schematics.

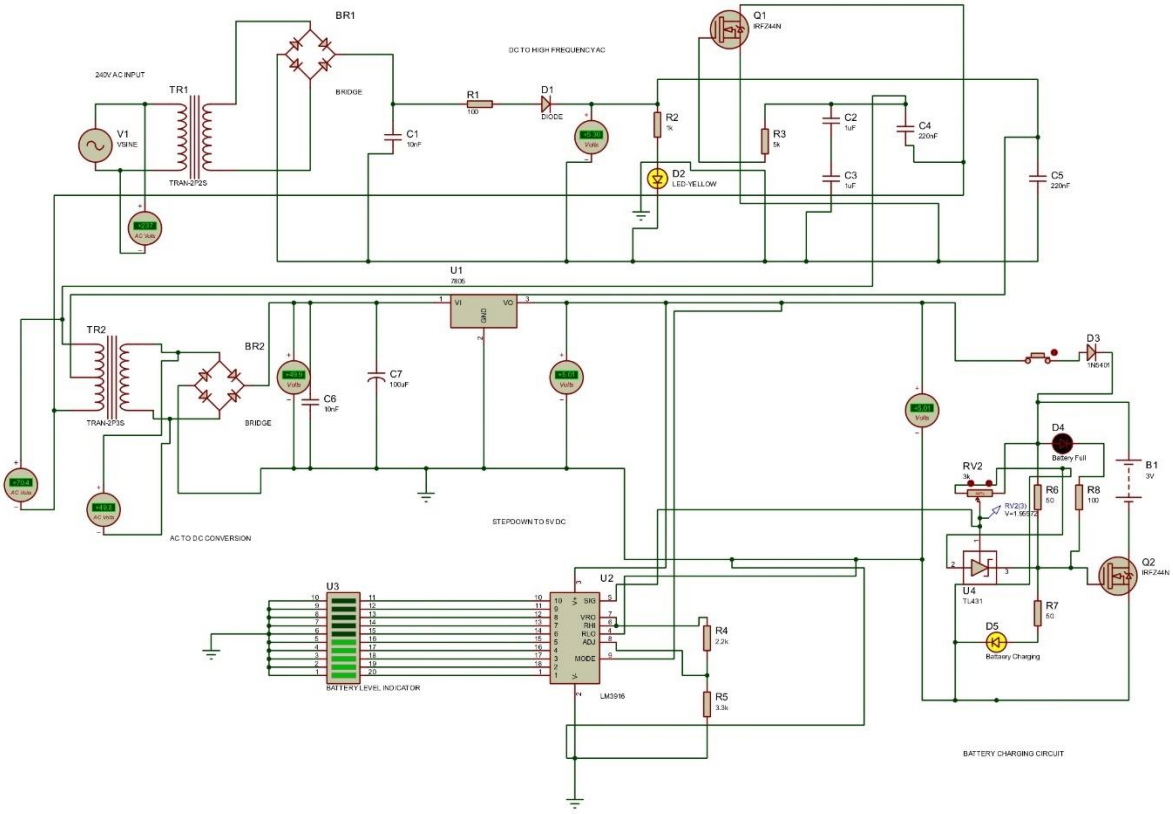

Figure 3.6: proteus Transmitter and Receiver with the battery management circuit and voltage level indicator showing a charging Battery.

In the above circuit, AC voltage is received from either the grid or the solar panel depending on availability. The AC voltage undergoes rectification by the bridge diode to Dc voltage. The DC is then converted from low-frequency DC into high-frequency AC. Here's how it works:

1. **MOSFET Switching:** The IRFZ44N MOSFET operates as an electronic switch. Its gate is driven by oscillations generated within the circuit, allowing it to alternately conduct and block current.

2. **Feedback Network**: The capacitors (C2, C3, C4, C5) and resistor (R3) form a feedback and timing network. These components determine the oscillation

frequency of the circuit. They allow the circuit to generate alternating signals at the gate of the MOSFET, creating high-frequency switching.

3. **Oscillation Mechanism:** When DC power is applied, the feedback network starts a self-sustaining oscillation. This creates a pulsed (alternating) voltage at the drain of the MOSFET, effectively converting the DC input to a high-frequency AC output.

4. **Capacitive Coupling:** The capacitors in the circuit assist in shaping the oscillation and ensuring proper phase alignment of the feedback signal to maintain stable operation.

At the receiving circuit, the ac is converted back to DC by the bridge circuit and further stepped down to 5volts by the 7805-voltage regulator that will later be used to charge the 3v lithium-ion battery.

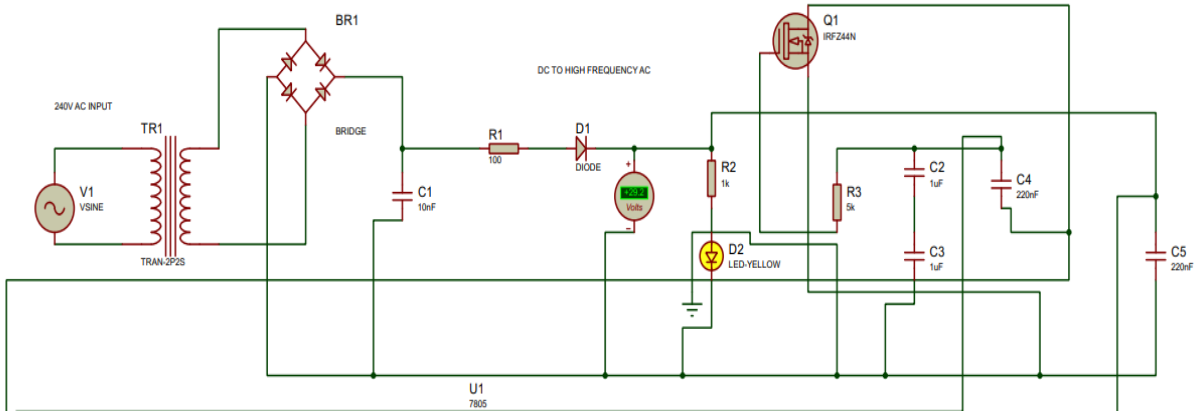

Figure 3.7: The Transmitter circuit

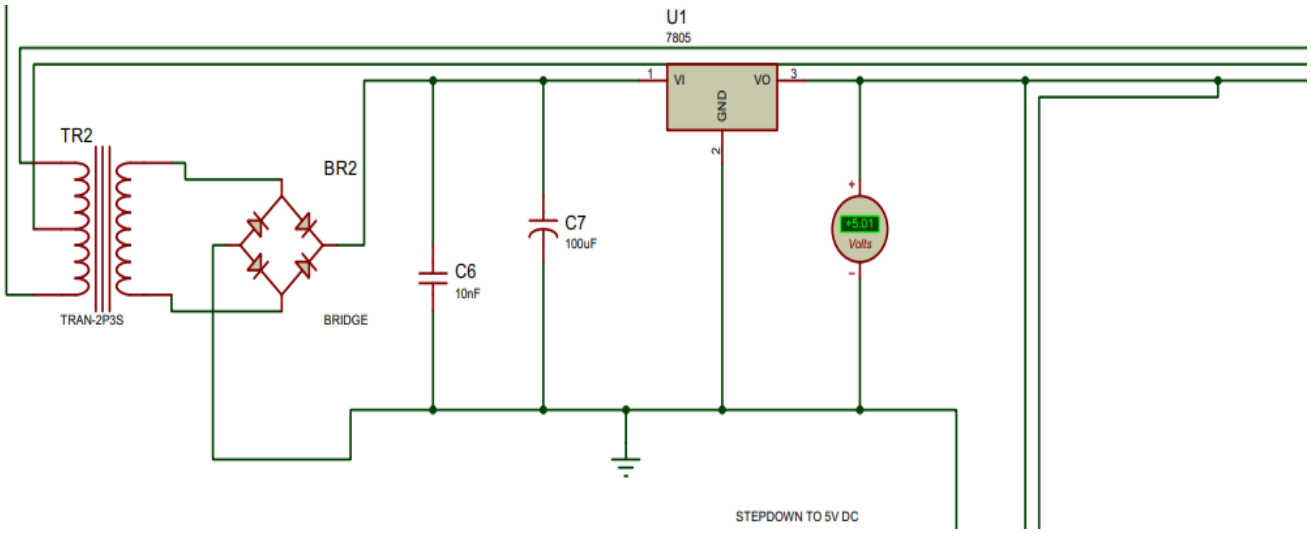

Figure 3.8: The receiver circuit.

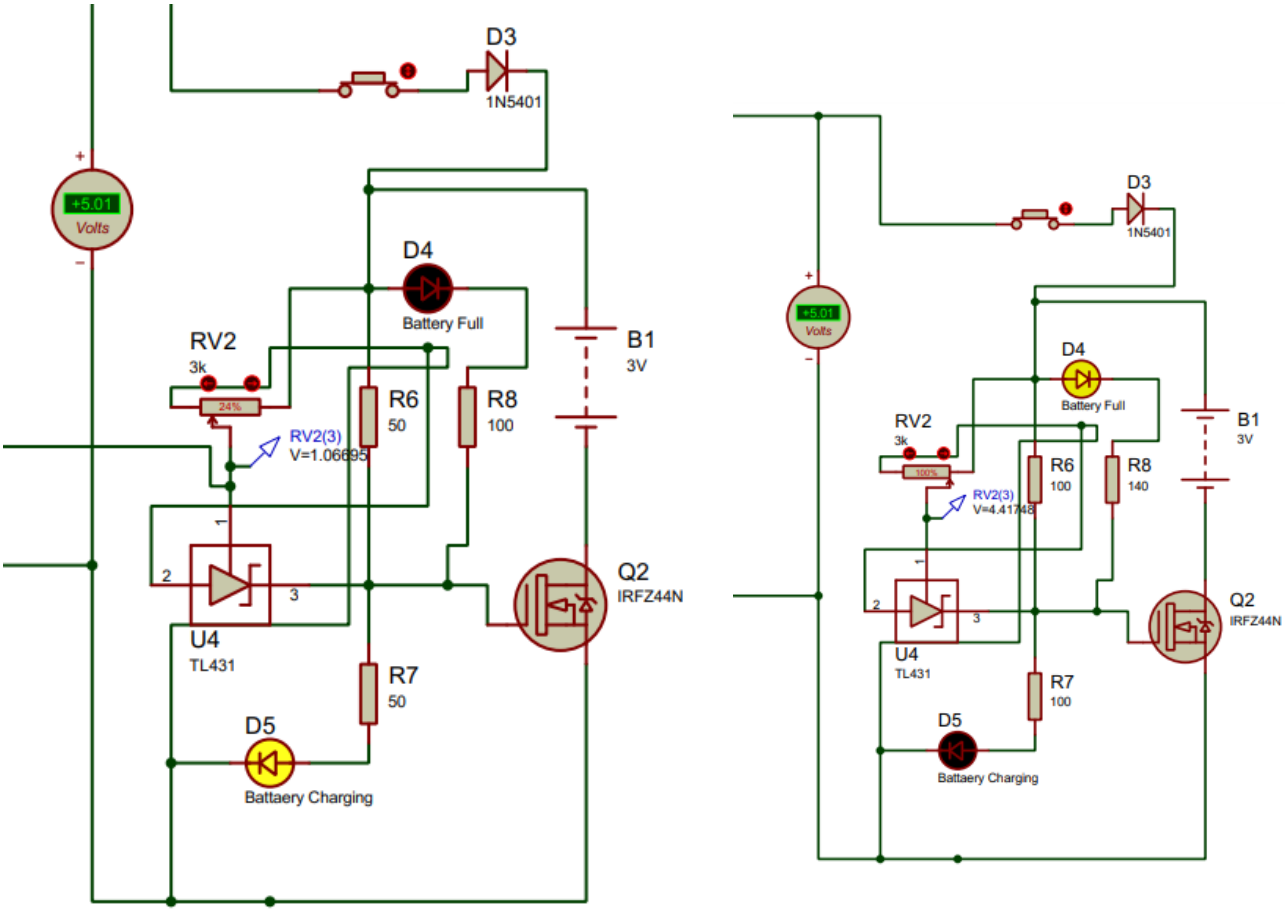

Figure 3.9: The battery charging circuit for charging status and fully charged status

The battery charging system is designed to regulate the charging of a 3V battery (B1). It incorporates a **MOSFET switch (Q2**), a shunt voltage reference (U4 - TL431), and various passive components to manage the charging process. Here's how it works:

1. Input Power Supply:

- The circuit is powered by a 5V DC input from the output of the transmitter.

2.Voltage Regulation:

-TL431 (U4): This is a programmable shunt voltage reference. It monitors the battery voltage through a **voltage divider** (formed by RV2 and R6) to determine when the battery is fully charged.

-RV2: This adjustable potentiometer sets the reference voltage, allowing the user to configure the charging cutoff voltage.

3.Charging Process:

- When the battery is not fully charged:

- The TL431 remains in a high-impedance state, keeping the MOSFET (Q2) turned on.

- The current flows through Q2 to charge the battery (B1).

- The **"Battery Charging" LED (D5)** lights up to indicate that charging is active.

4.Full-Charge Detection:

- When the battery voltage reaches the set threshold:

- The TL431 turns on (low impedance) and sinks current, reducing the gate voltage of the MOSFET (Q2).

- This action turns off Q2, stopping the charging process.

- The "**Battery Full" LED (D4) lights up, indicating the battery is fully charged**.

5.Protection Components:

-D3 (1N5401): This diode protects the circuit from reverse voltage or polarity mistakes.

- R6, R7, R8: These resistors control the current flow and stabilize the operation of the circuit.

Key Features of the batter management system

- Overcharging Protection: The circuit ensures the battery stops charging when it reaches the specified voltage to prevent overcharging.

- **Adjustable Voltage Threshold**: The potentiometer (RV2) allows customization and simulation of real time charging and discharging.

- **Status Indication**: LEDs indicate the charging state (charging or full).

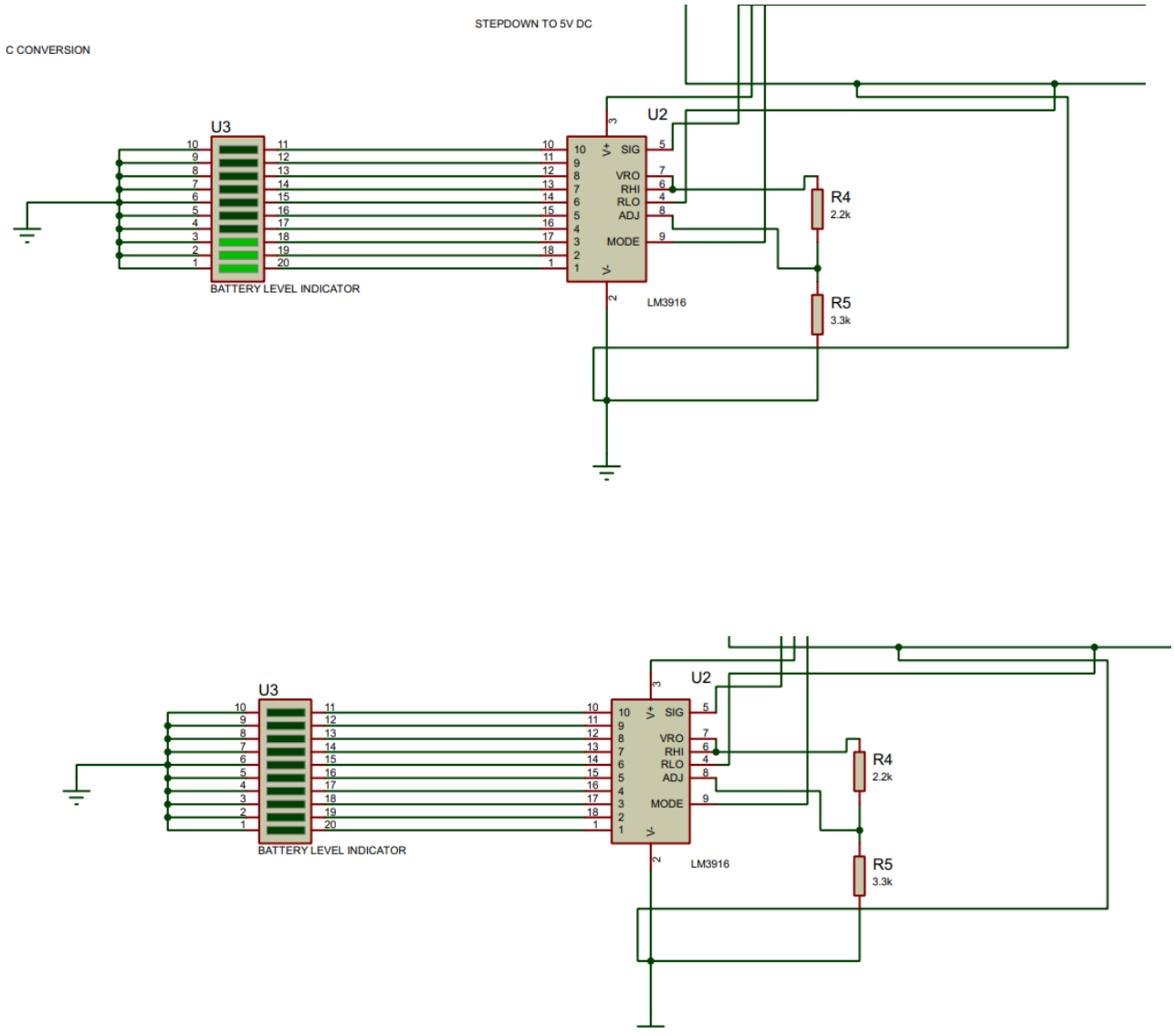

Figure 3.10: Battery level indicator for various voltage levels

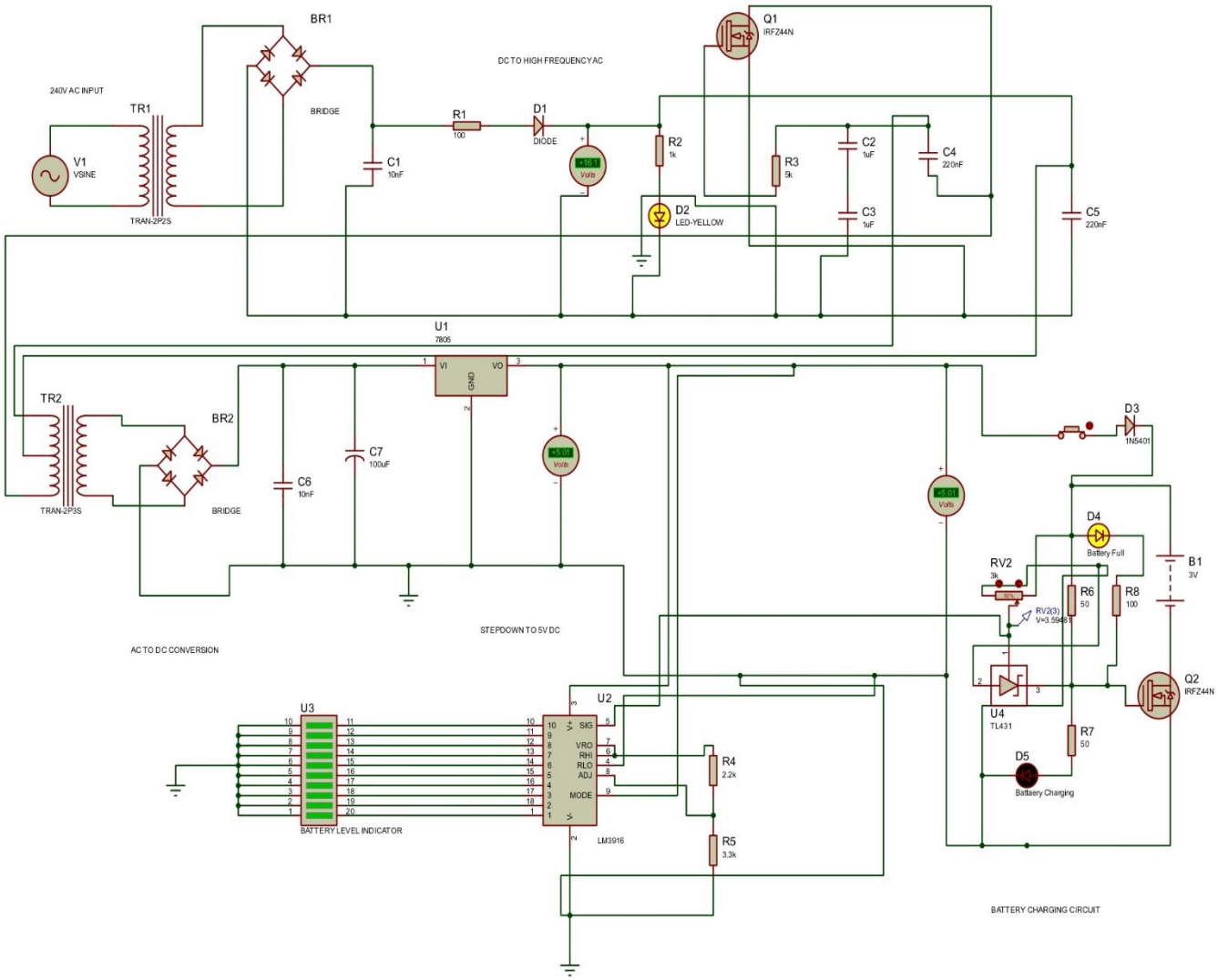

Figure 3.11: Full battery voltage circuit achieved by induction

The above schematic shows a fully charged battery which the battery management system has in turn disconnected from the circuit.

Solar power circuit, grid power circuit, charging station load control and automatic change over between solar and grid depending on availability for uninterrupted power supply to the station

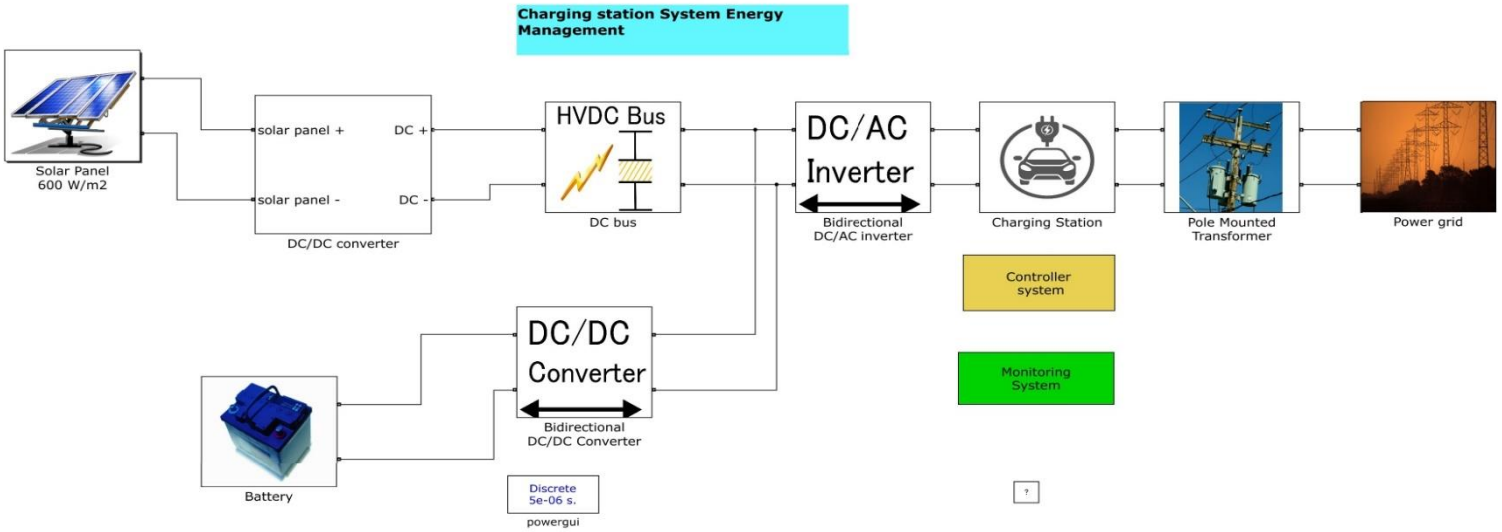

Figure 3.12: solar circuit.

The above system has been designed to operate in subsystems within the individual blocks. That is the panel subsystem, DC/DC converter subsystem, DC bus system, Bidirectional DC/AC inverter subsystem, Bidirectional DC/DC converter subsystem, the Battery subsystem, the charging station, the pole mounted transformer and the power grid.

3.4 The solar subsystem

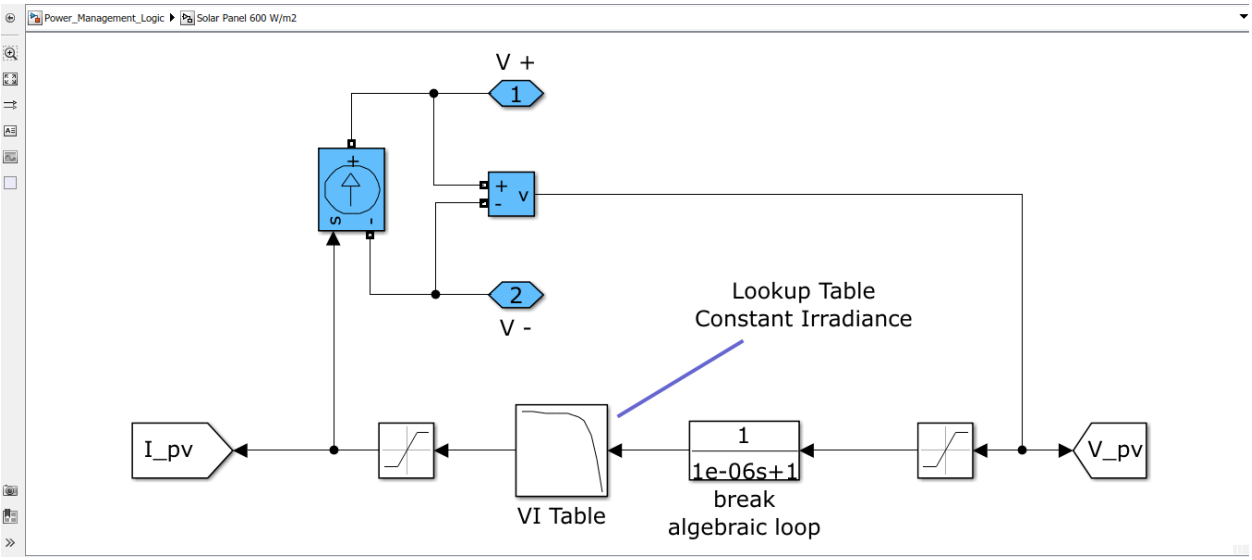

Figure 3.13: The solar subsystem

The solar panel subsystem diagram shown is a model of a photovoltaic (PV) panel's operation under constant irradiance. Here's an explanation of its components and working:

The system includes key components to measure and simulate the solar panel's performance. Voltage sensors (V+ and V-) measure the panel's voltage (V_pv), while a current sensor (I_pv) measures the generated current. A lookup table (VI Table) uses the panel's voltage (V_pv) to determine the corresponding current (I_pv) based on the solar panel's I-V curve under constant sunlight. To avoid simulation issues caused by algebraic loops, a block with a small time constant ensures numerical stability. The measured voltage is fed back into the VI Table to update the current, and the system calculates the panel's output power ($P = V_{pv} \times I_{pv}$) from the feedback of voltage and current.

3.5 DC-DC CONVERTER CIRCUIT

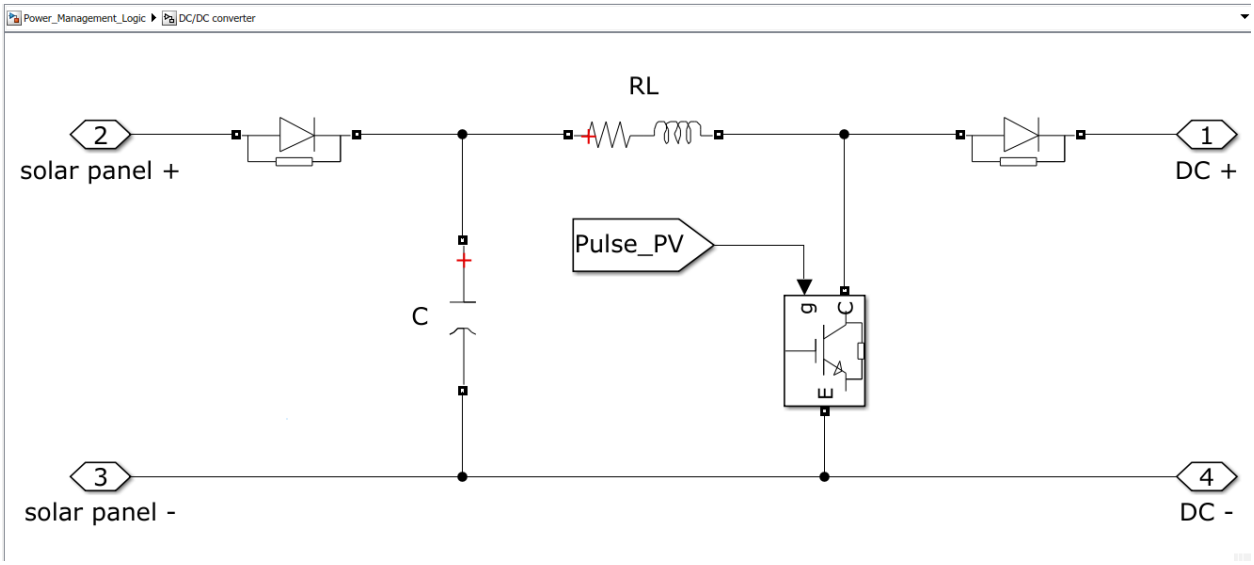

Figure 3.14: dc dc converter circuit

This DC-DC converter circuit represents a boost converter designed to step up the voltage from a solar panel to a higher DC output voltage.

The circuit uses key components to manage and regulate the flow of energy from a solar panel. Diodes ensure current flows in one direction: the left diode prevents reverse flow to the panel, and the right diode stops backflow from the output. A capacitor smoothens the output voltage and stores energy, while an inductor stores energy as a magnetic field and helps boost voltage. A transistor (IGBT) acts as a switch, controlled by a PWM signal (`Pulse_PV`) that adjusts the duty cycle to regulate the output voltage. When the transistor is ON, current flows through the inductor, storing energy in its magnetic field while the right diode blocks discharge from the capacitor. When the transistor is OFF, the stored energy from the inductor flows through the right diode into the capacitor and load, boosting the output voltage. By adjusting the PWM signal, the circuit ensures the output voltage remains higher than the input.

3.6 DC BUS

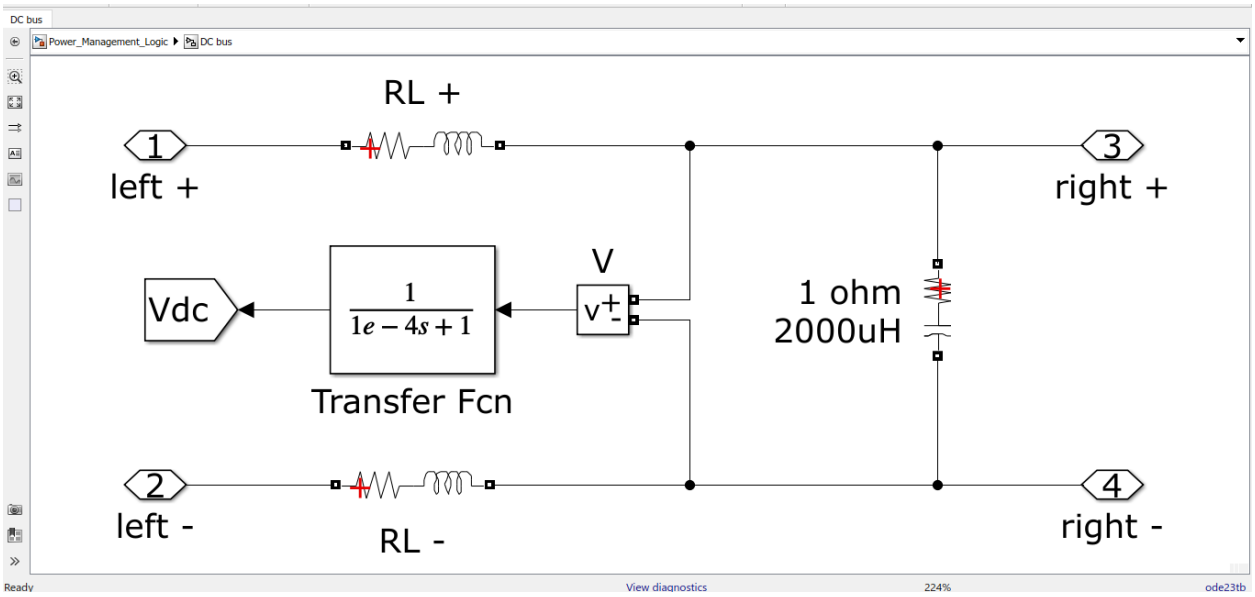

Figure 3.15: DC BUS

This circuit illustrates the workings of a DC bus system, where energy transfer and voltage regulation are achieved using inductors, resistors, and control blocks.

Key Components and their Roles:

1.Input Ports (Left + and Left -):

- The left-side terminals represent the input power source, typically from a DC supply.

2.Series RL Components:

- The series-connected resistor RL+ and inductor on the positive side and RL- on the negative side represent the parasitic resistances and inductances of the cables or connections in the system.

The system's transfer function,

$$\frac{1}{1e-4s+1} \qquad (1)$$

,

represents the control dynamics of a voltage regulator designed to stabilize the output voltage (Vdc). This first-order low-pass filter smooths high-frequency noise while allowing slower variations to pass. Voltage measurement ensures the bus voltage remains within set parameters.

The DC bus output, provided through the right-side terminals, delivers regulated power to downstream systems. Energy flows through RL+ and RL-, accounting for losses and energy storage in transmission lines. Feedback from the voltage measurement block helps the transfer function regulate Vdc, stabilizing it against load or input fluctuations. The connected load includes a 1-ohm resistor for energy dissipation and a 2000 µH inductor for temporary energy storage and delayed current changes, defining the load's dynamic response. The DC bus acts as an intermediary, delivering smooth, stable power and countering disturbances through feedback control and reactive components.

3.7 BIDIRECTIONAL DC/AC INVERTER.

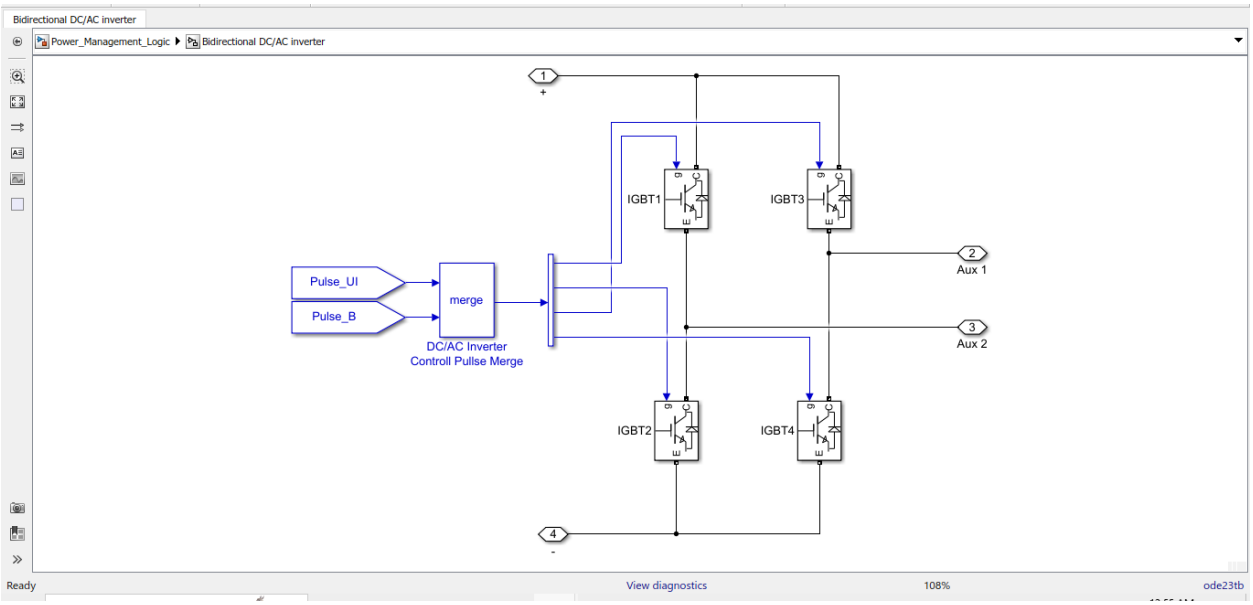

Figure 3.16: Bidirectional DC/AC inverter

A bidirectional DC/AC converter allows the conversion of power between DC and AC in both directions, facilitating applications such as renewable energy systems, energy storage, and grid interaction.

The system includes key components for efficient power conversion. Control signals (Pulse_UI and Pulse_B) are generated by a controller to manage the switching devices. A merge block combines these signals to drive the gate of four IGBTs (switches) arranged in an H-bridge configuration, allowing bidirectional power flow between DC and AC. Terminals 1 and 4 handle DC input/output, while Terminals 2 and 3 manage AC input/output. In inverter mode, the system converts DC to AC, creating an AC waveform at the output using Pulse Width Modulation (PWM) to control frequency and amplitude. In rectifier mode, it converts AC to DC, providing smooth DC output. The system supports

bidirectional energy flow, ideal for integrating renewable energy sources, connecting DC to AC grids, and managing energy storage systems for charging and discharging.

3.8 BIDIRECTIONAL DC/DC CONVERTER

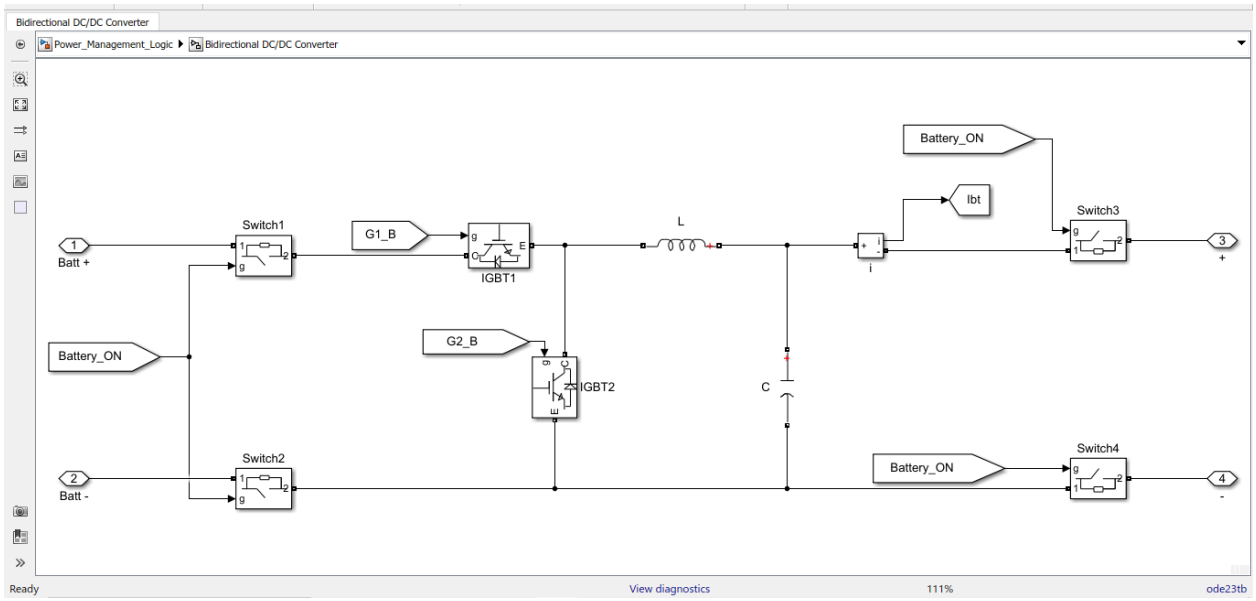

Figure 3.17: Bidirectional DC/DC converter

The converter system includes key components: switches (Switch1–Switch4) control power direction, an inductor (L) stores and transfers energy, and a capacitor (C) stabilizes the DC bus voltage by reducing ripples. IGBTs (IGBT1 and IGBT2) are the main switching devices, and the Battery_ON signal manages the switches to enable power flow.

The converter operates in two modes: **Battery Charging Mode,** where power flows from the DC bus to the battery, and **Battery Discharging Mode**, where the battery supplies power to the DC bus. In charging mode, Switch1 and Switch2 alternate, with the inductor storing energy via IGBT1 and releasing it to the battery via IGBT2, supported by the capacitor for voltage stability. In discharging mode, Switch3 and Switch4 alternate, with the inductor transferring energy from the battery to the DC bus, regulated by the IGBTs and stabilized by the capacitor.

3.9 CHARGING STATION

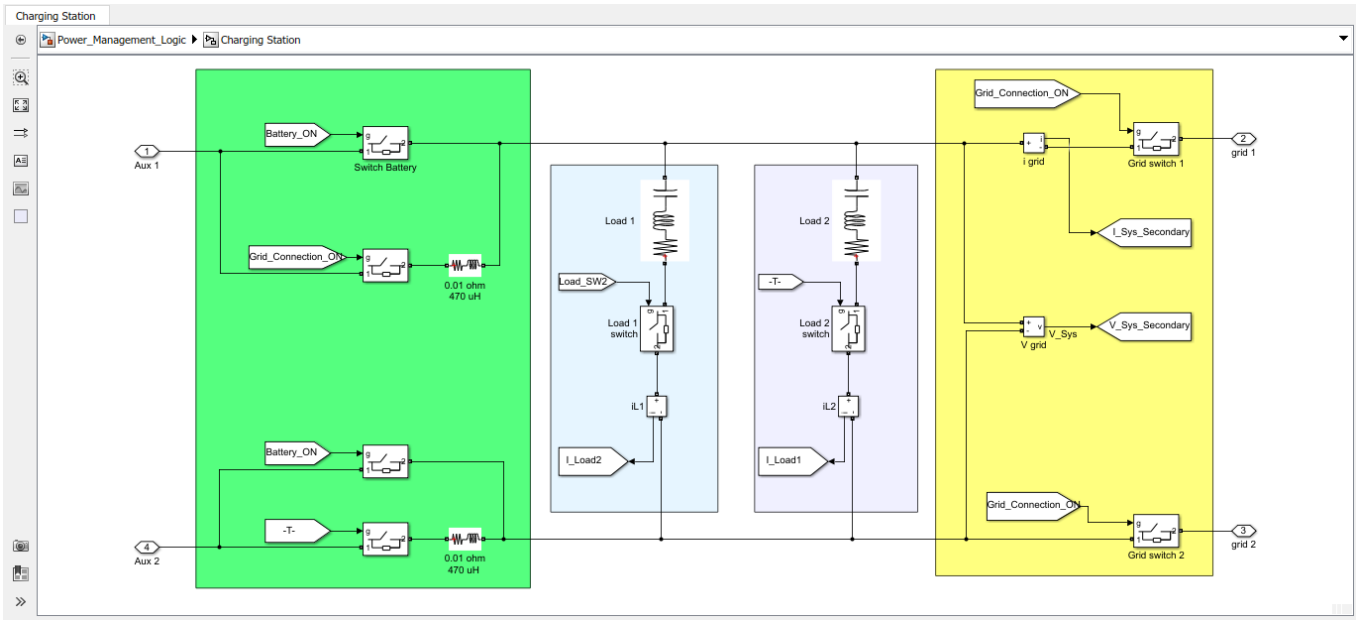

Figure 3.18: Charging Station

This circuit represents a charging station system with automatic changeover between grid and battery (solar-backed) power, with grid power as the priority source. Two loads represent the charging spots in the station.

The system manages power distribution between a grid and a battery, ensuring uninterrupted operation. The **Battery System** (Green Block) includes a Battery_ON switch to connect the battery, an inductor (470 µH) to smooth current flow, and switches for grid connection. Auxiliary inputs (Aux1, Aux2) provide additional battery inputs. The **Load System** (Blue and Purple Blocks) has two charging spots (Load 1, Load 2), each controlled by switches (Load_SW1, Load_SW2) and monitored by current sensors (iL1, iL2). The **Grid System** (Yellow Block) supplies power via Grid Switches 1 and 2, with sensors (V_Sys and i_grid) monitoring voltage and current.

Modes of Operation:

1. Normal Operation (Grid Priority): When the grid is active, power flows through Grid Switches 1 and 2 to the loads, while the battery remains idle. Sensors monitor grid stability.

2. Backup Operation (Battery Power): During grid failure, the Battery_ON switch activates, delivering power through the inductor to the loads. Current sensors ensure smooth operation.

Key Features: The system prioritizes grid power, uses the battery as a reliable backup during outages, allows independent control of charging spots, and transitions automatically between grid and battery power, ensuring seamless operation.

3.10 EXTERNAL SOURCES i.e., Power from the grid

Pole mounted transformer.

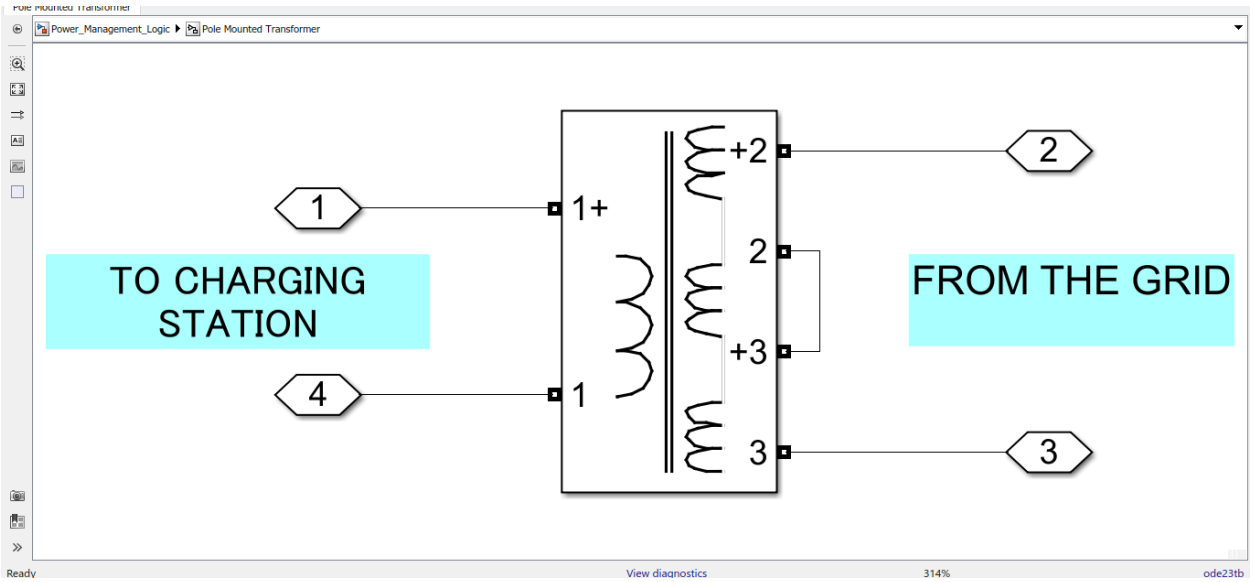

Figure 3.19: Pole Mounted Transformer

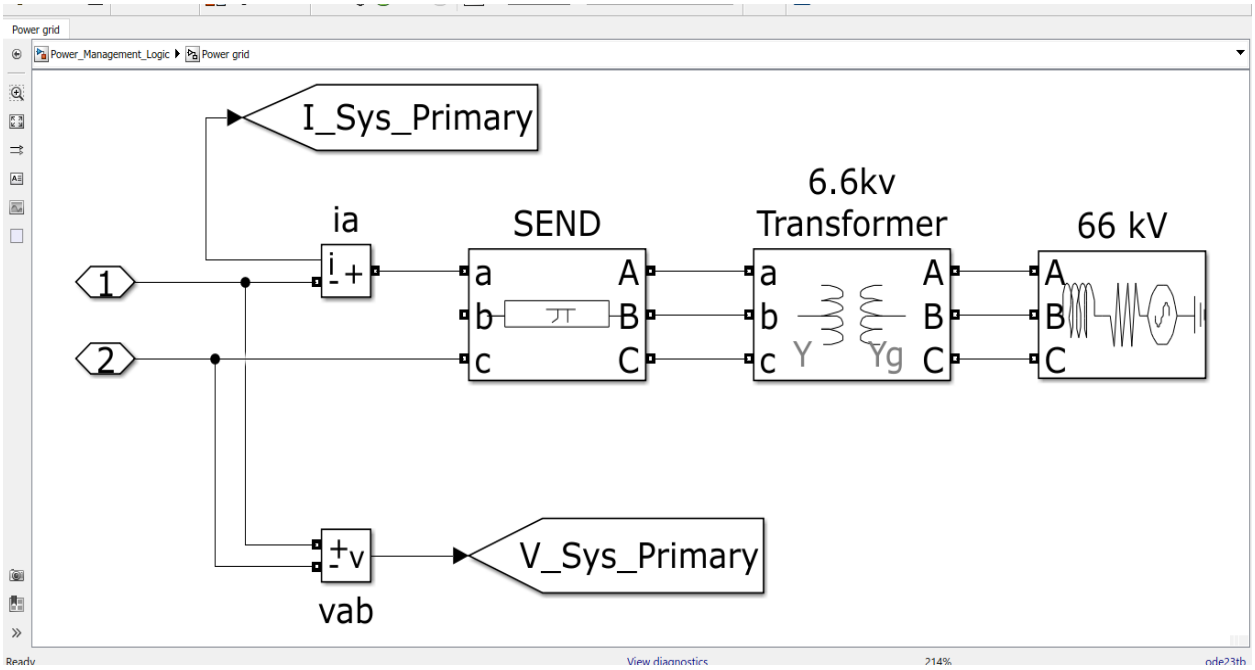

Figure 3.20: The Grid

1.66 kV Transmission Grid:

- The 66 kV grid supplies cpa high-voltage power for long-distance transmission.

- This power is input into the 6.6 kV transformer, which steps the voltage down from 66 kV to 6.6 kV.

- This step is necessary to transition the voltage from the high-voltage grid to a distribution-level voltage suitable for local systems.

2. 6.6 kV Local Distribution System:

- The stepped-down 6.6 kV power is then delivered to the local distribution network through a short transmission line represented by the SEND block (π-equivalent circuit).

- This 6.6 kV system is fed into the pole-mounted transformer.

3. Pole-Mounted Transformer:

- The pole-mounted transformer further steps down the voltage from 6.6 kV to a lower voltage, typically 240 V, as per the requirements of the EV wireless charging station.

4. EV Wireless Charging Station:

- The low-voltage output from the pole-mounted transformer powers the EV wireless charging station.

At the charging station:

- The power is converted into high-frequency AC to generate a magnetic field.

- The EV receives this power wirelessly through its onboard receiver coil.

3.11 THE CONTROL SYSTEM

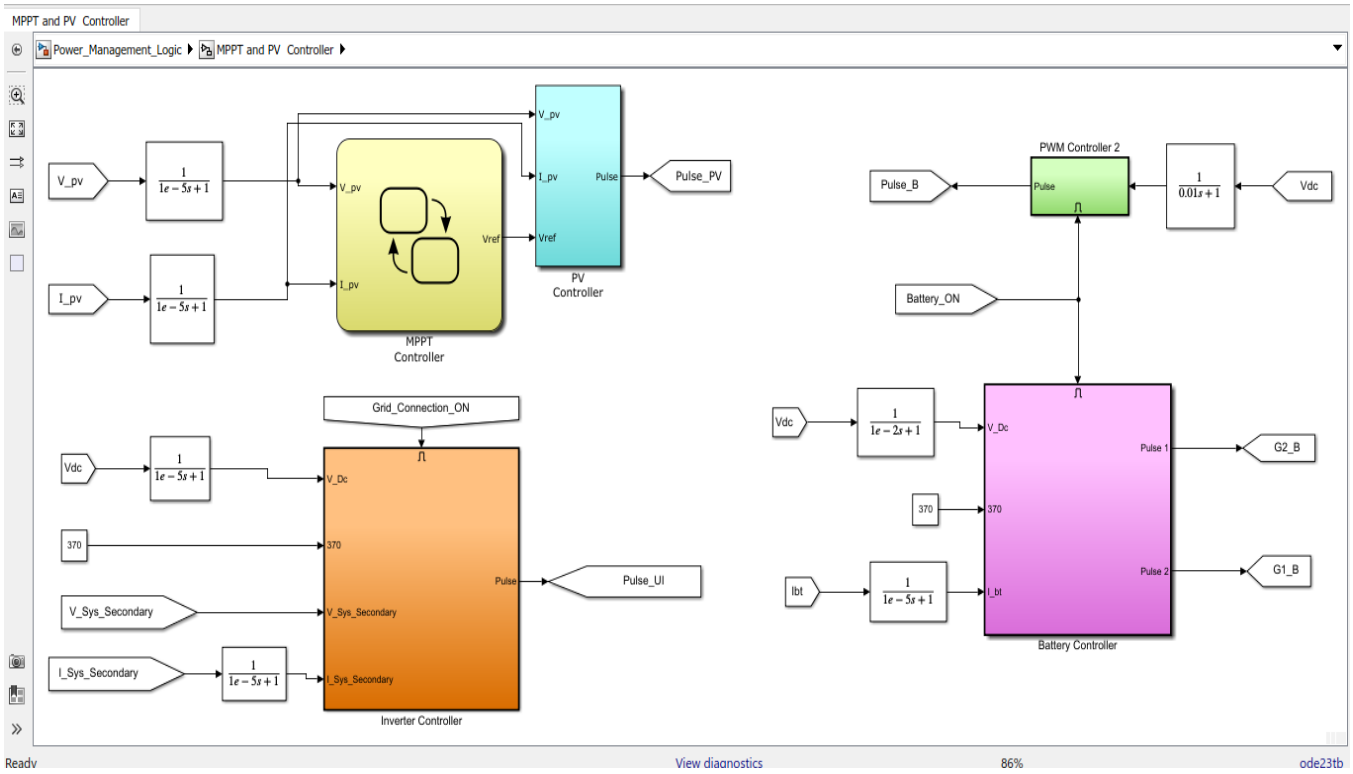

Figure 3.21: control system

The block diagram represents a hybrid control system for integrating solar photovoltaic (PV) power and a grid system to manage energy flow efficiently.

The system consists of inputs, controllers, and outputs that work together to manage energy flow in a hybrid solar power setup. Inputs include PV voltage (V_pv) and

current (I_pv), used by the MPPT controller to maximize power extraction, and DC bus voltage (V_dc) with battery current (I_bt), which guide the battery controller.

The MPPT controller determines the optimal operating point for the PV panel and provides a reference voltage (V_ref) for the PV controller, which generates a Pulse_PV signal to drive a DC-DC converter.

The inverter controller manages DC voltage (V_dc), synchronizing with the grid or supporting local loads, while the battery controller ensures proper charging and discharging via Pulse 1 and Pulse 2 signals.

A PWM controller generates additional pulse signals for power devices. Logic signals, Grid_Connection_ON and Battery_ON, guide system operation for grid interaction and battery management.

Outputs like Pulse_PV, Pulse_UI, and battery pulses facilitate solar generation, battery management, grid integration, and hybrid operation. Low-pass filters ensure smooth operation across all controllers.

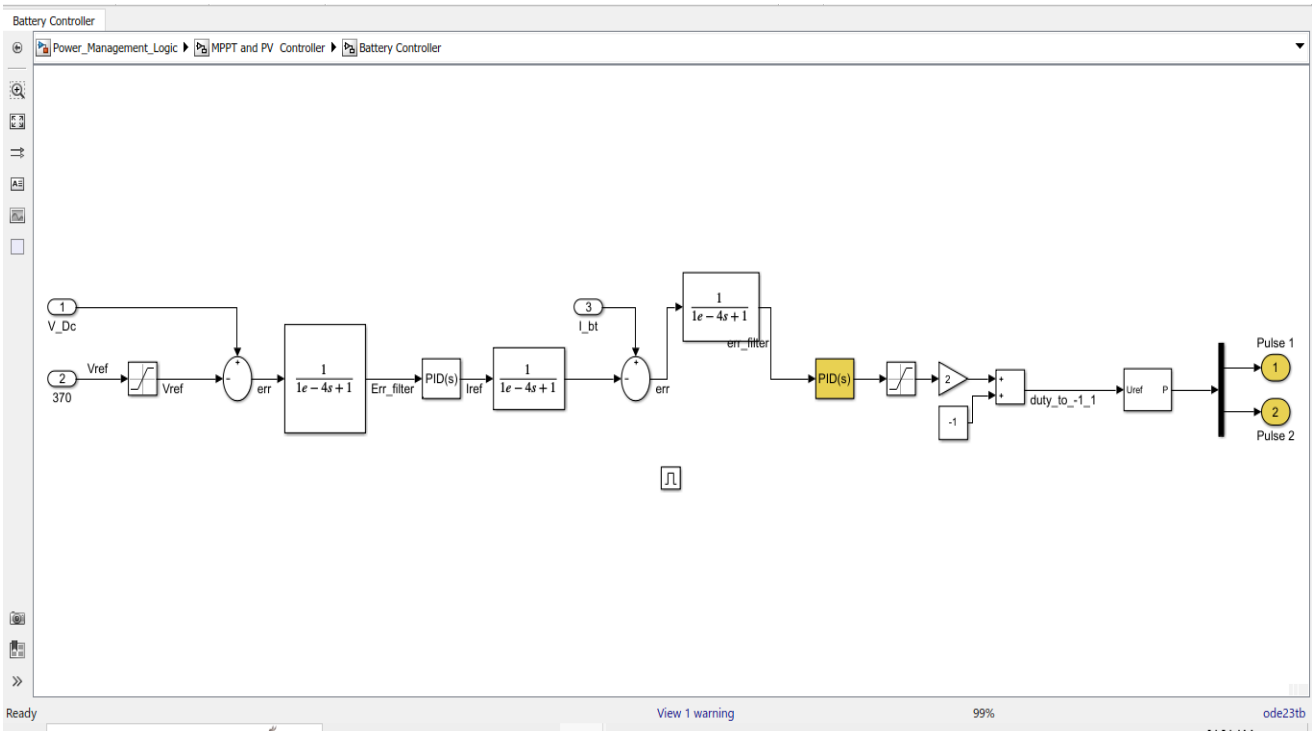

Figure 3.22: Battery controller

This Simulink block diagram represents a battery controller that regulates the system voltage and current.

The system employs a two-loop control strategy to manage the battery's state and regulate the DC voltage. The voltage control loop ensures the DC voltage (V_Dc) matches a desired reference (V_ref) by computing the error, filtering it to reduce noise, and processing it through a PID controller to generate a reference current (I_ref). The current control loop adjusts the battery current (I_bt) to follow I_ref by computing the error, filtering it, and using another PID controller to produce a duty cycle command. This duty cycle is scaled, limited, and converted into control signals for a PWM generator, which outputs pulses (Pulse 1 and Pulse 2) to control the system's switches or converters. Together, these loops maintain stable DC voltage, regulate battery current, and ensure efficient power system operation.

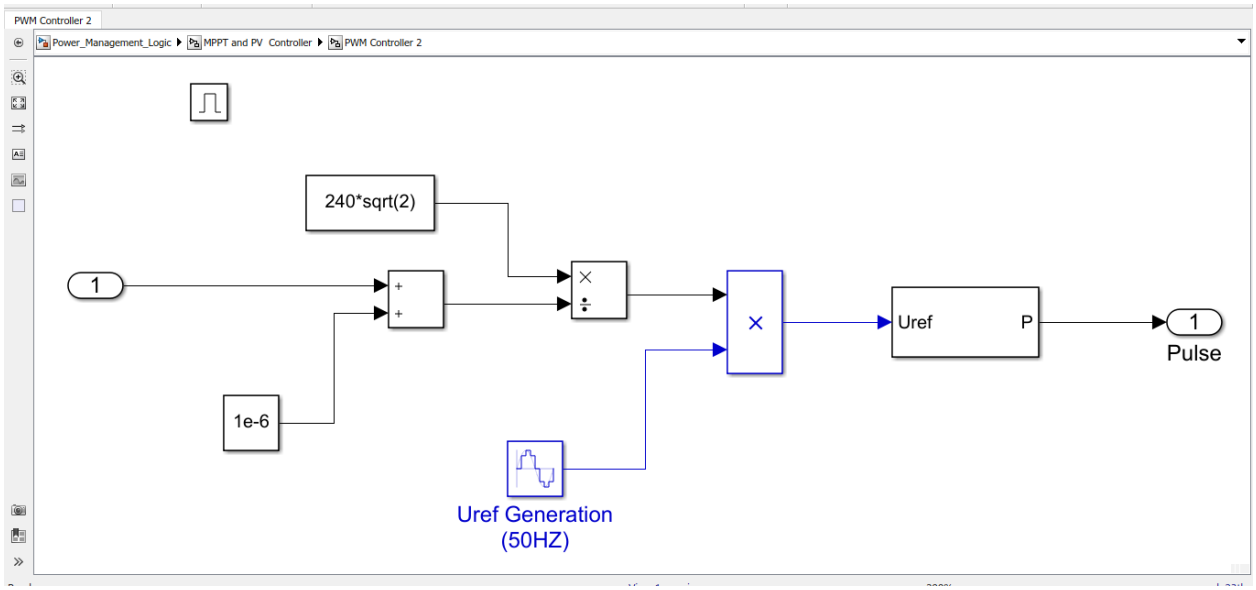

Figure 3.23: Pulse controller

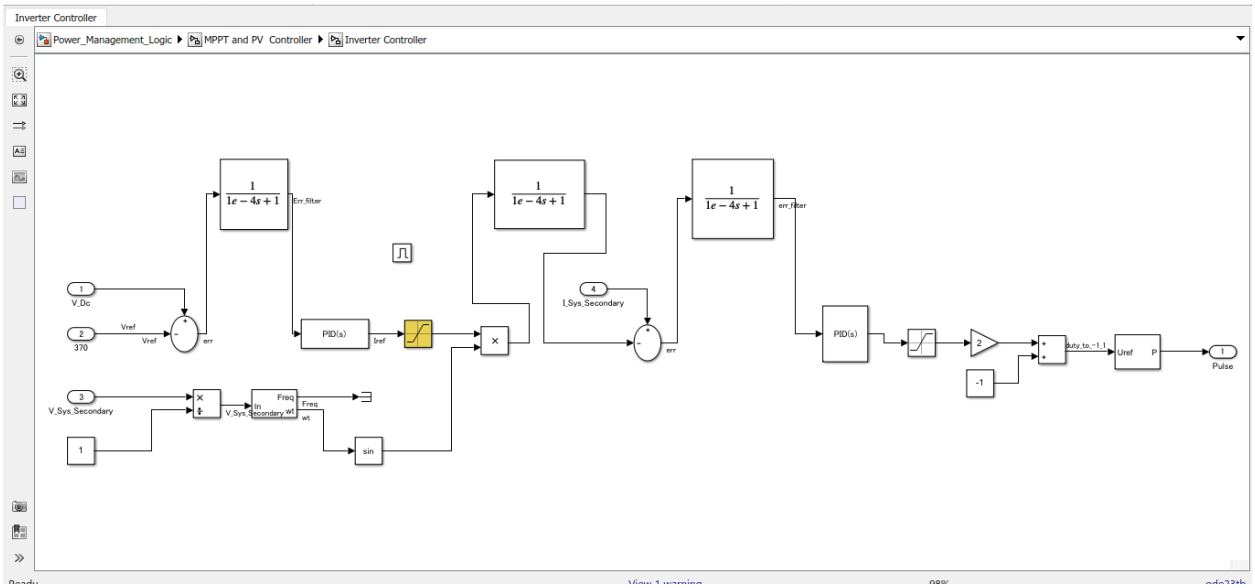

Figure 3.24: inverter controller

This diagram represents a closed-loop inverter controller with voltage and current regulation.

The system features a voltage feedback loop, current feedback loop, and PWM generator to regulate DC voltage and produce sinusoidal AC output. The voltage loop compares the DC bus voltage (VDC) with a reference (Vref, 370V), filters the error to reduce noise, and uses a PID controller to generate a current reference (Iref). The current loop compares the actual system current with Iref, filters the error, and processes it through another PID controller to create a control signal. A sine wave reference is generated for AC modulation, combining the control signal to produce a sinusoidal voltage reference. The duty cycle is calculated to fit the PWM range and fed to a PWM generator, which drives the inverter switches. This setup maintains the desired DC voltage, produces clean sinusoidal AC output, and minimizes current distortion.

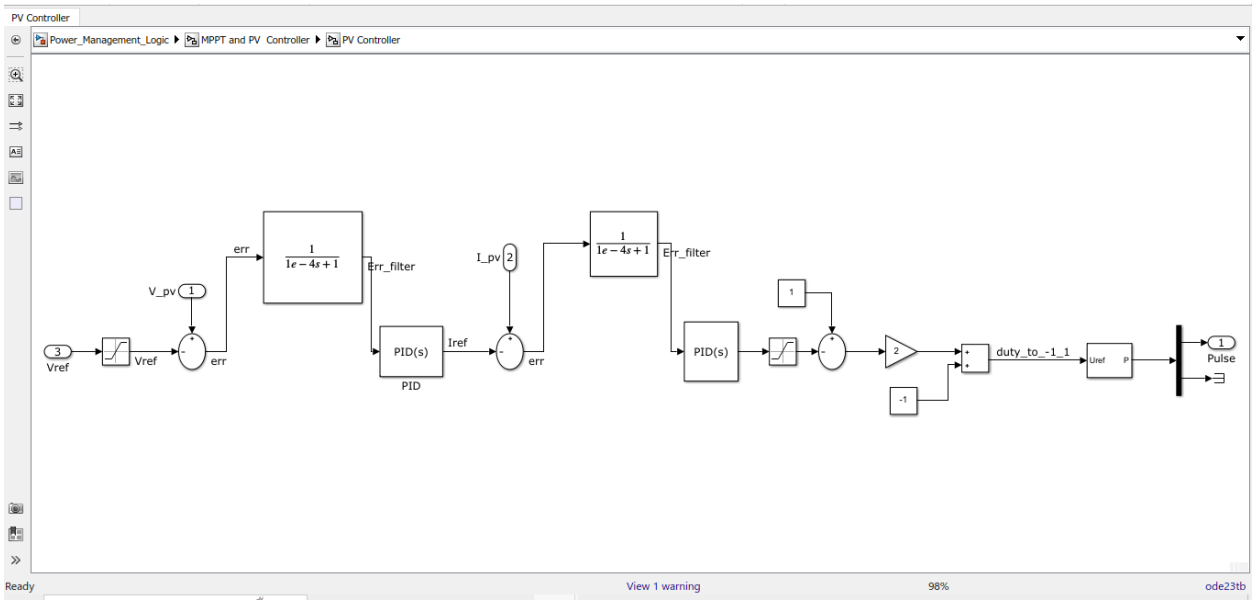

Figure 3.25: PV controller

This block diagram represents a photovoltaic (PV) controller designed for Maximum Power Point Tracking (MPPT) and maintaining stable PV system output.

The system regulates the PV system's voltage and current using a voltage control loop, current control loop, and PWM generation. The voltage loop compares the reference voltage (V_ref) with the actual PV voltage (V_pv) to calculate an error, which is filtered to remove noise and processed by a PID controller to produce a reference current (I_ref). The current loop compares I_ref with the actual PV current (I_pv), filters the error, and uses another PID controller to generate a control signal. This signal is squared, adjusted, and converted into a duty cycle ranging from -1 to 1, which drives a PWM generator. The PWM output produces pulses to control the PV system's power electronics, ensuring stable operation and efficient power extraction. Low-pass filters and PID controllers play a key role in maintaining desired voltage and current levels, while PWM generation translates control signals into actionable switching commands.

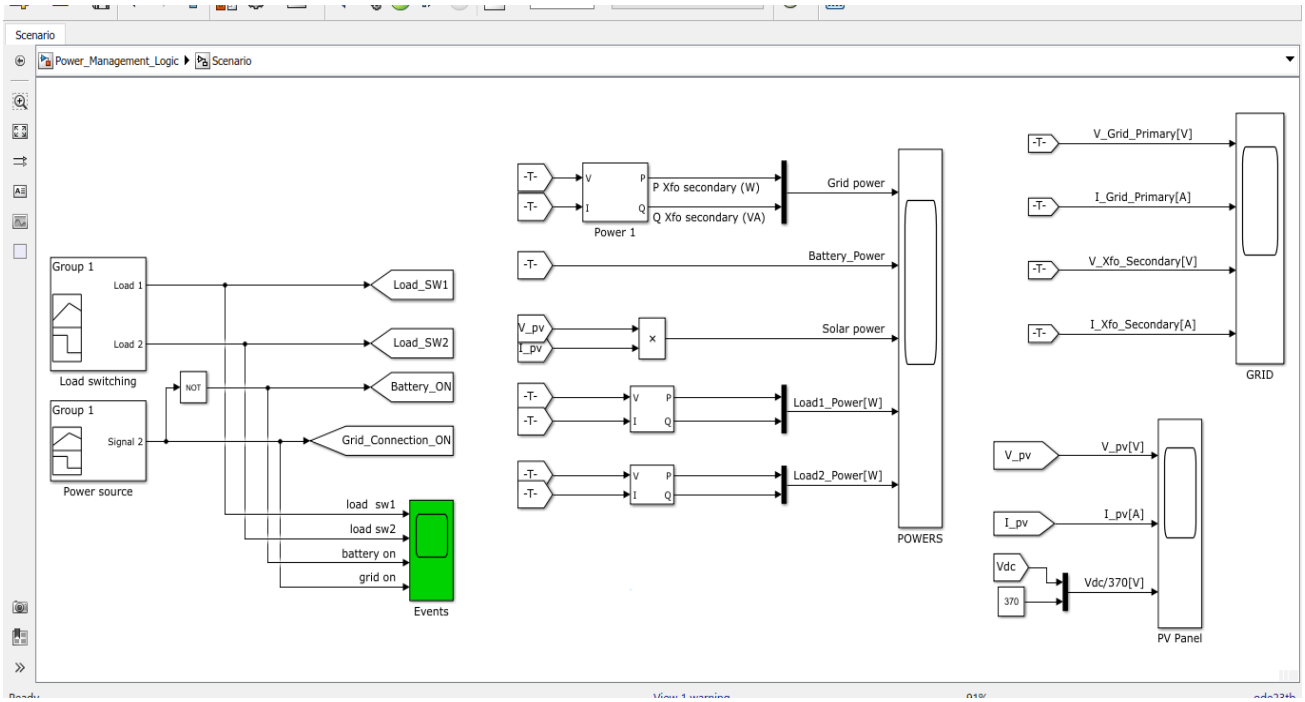

Figure 3.26: Monitoring system

3.12 State of Charge (SoC) Overview

State of Charge (SoC) represents the amount of charge remaining in a battery, often expressed as a percentage:

• 100% SoC means the battery is fully charged.

• 0% SoC means the battery is empty.

SoC is commonly estimated using the voltage of the battery, although the relationship between voltage and SoC is not perfectly linear. Therefore, advanced methods like the Extended Kalman Filter (EKF) can improve the estimation accuracy

3.13 Simple Voltage-to-SoC Mapping

The voltage of the battery can be used to estimate the SoC. This assumes that the battery voltage varies linearly with the SoC.

Given:

• Vmax = maximum voltage (fully charged),

• Vmin = minimum voltage (fully discharged),

• Vmeasured = current measured voltage.

The formula for SoC is:

$$\text{SoC} = \frac{V_{\text{measured}} - V_{\text{min}}}{V_{\text{max}} - V_{\text{min}}} \qquad (2)$$

For example, if:

• Vmeasured = 12.0V,

• Vmax = 12.6V,

• Vmin = 9.0V,

then the SoC is:

$$\text{SoC} = \frac{12.0-9.0}{12.6-9.0} = \frac{3.0}{3.6} = 0.83 \quad \text{or} \quad 83$$

This is a basic estimation but does not consider other factors affecting the battery's behavior.

3.14 Extended Kalman Filter (EKF) for SoC Estimation

To improve the accuracy of SoC estimation, especially when voltage readings are noisy or unreliable, we use the Extended Kalman Filter (EKF). The EKF combines predictions based on a model with actual measurements, adjusting the SoC estimate as new data arrives.

Step 1: Predict the Next SoC

The EKF predicts the next SoC using the previous SoC and a model of the battery's behavior. The predicted voltage is given by:

$$\widehat{V_{\text{predicted}}} = V_{\min} + (V_{\max} - V_{\min}) \times \widehat{\text{SoC}_k} \qquad (3)$$

where SoCˆ k is the predicted SoC

Step 2: Measure the Actual Voltage

The actual voltage, Vmeasured, is measured, and we compare it with the predicted voltage.

Step 3: Update SoC Estimate

the difference between the predicted and measured voltage is used to update the SoC estimate. The Kalman Gain, K, determines the confidence we place in the new measurement compared to the prediction. It is calculated as:

$$K = \frac{P_k}{P_k + R} \qquad (4)$$

where:

- Pk is the uncertainty in the predicted SoC (error covariance),
- R is the uncertainty in the measured voltage.

$$\widehat{\text{SoC}_k} = \widehat{\text{SoC}_k} + K \times \left(V_{\text{measured}} - \widehat{V_{\text{predicted}}}\right) \qquad (5)$$

Step 4: Update the Uncertainty

The error covariance, $P_{k,}$ is updated as follows to reflect the reduced uncertainty:

$$P_k = (1 - K) \times P_k \qquad (6)$$

this adjustment helps to refine future estimates based on the relative confidence in measurements.

CHAPTER 4: RESULTS AND DISCUSSIONS

4.1 Solar power and Grid Power Change over switching.

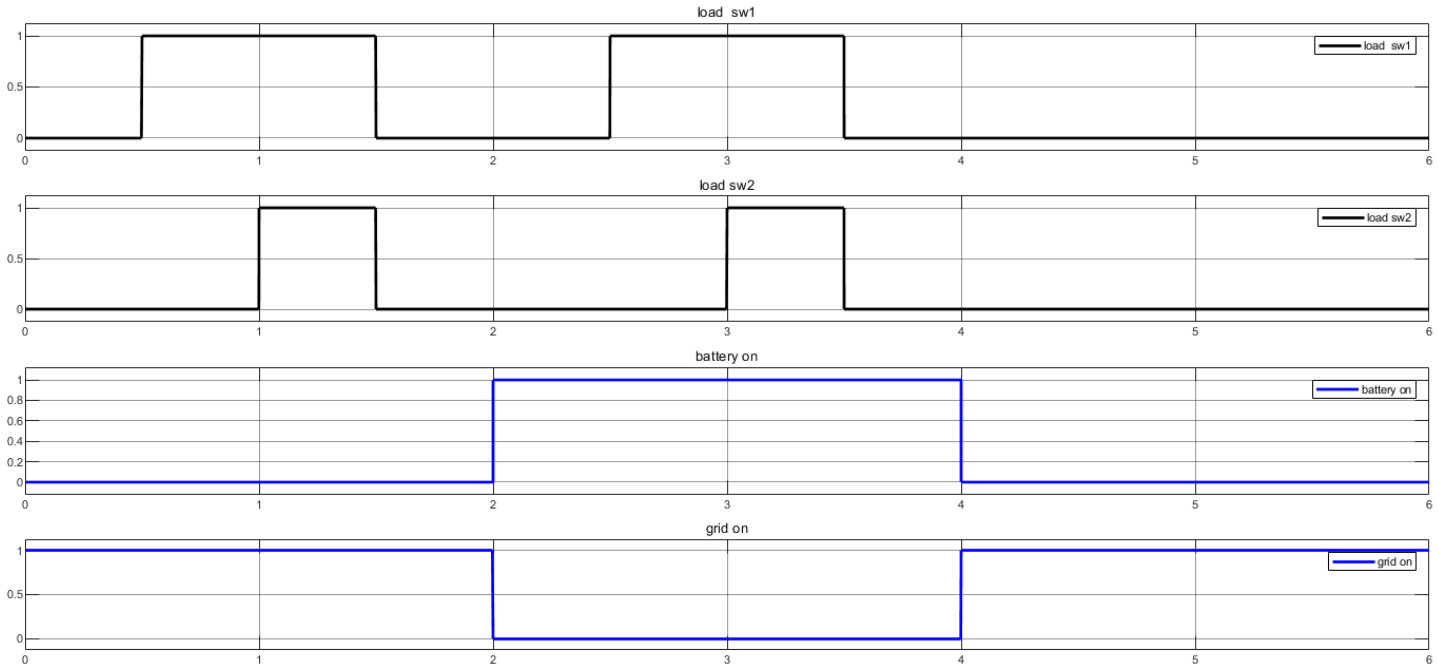

Figure 4.1: Battery solar Change Over

As it can be seen when the grid power falls from high to low, the battery storage from the solar system picks on.

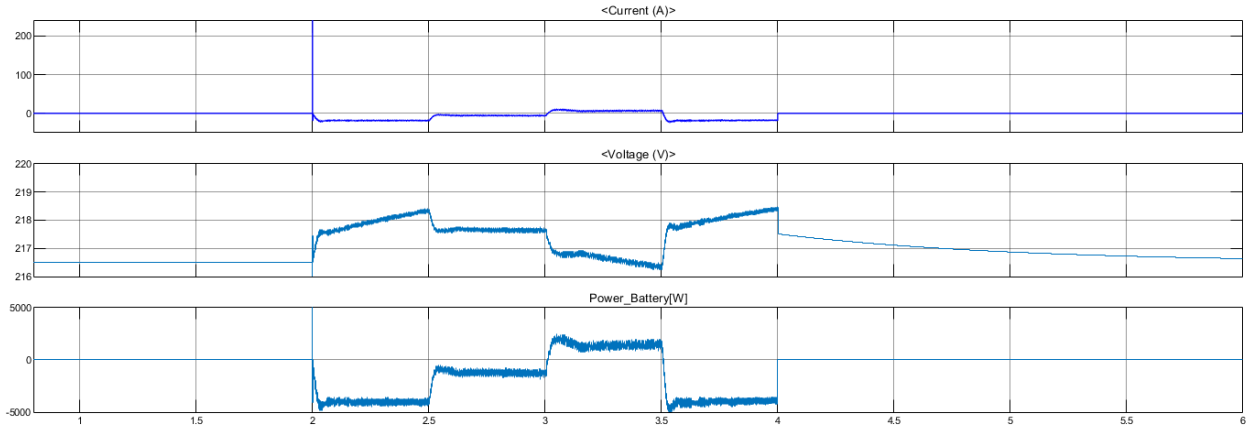

Figure 4.2: Battery voltage power and current during the discharging process

The above graph illustrates the smooth transition of power from the grid to the solar system. When the grid goes down, the system quickly adjusts to maintain power delivery using solar energy or batteries, as seen by the current and power stabilizing after the brief disruption.

4.2 Power outputs and load power

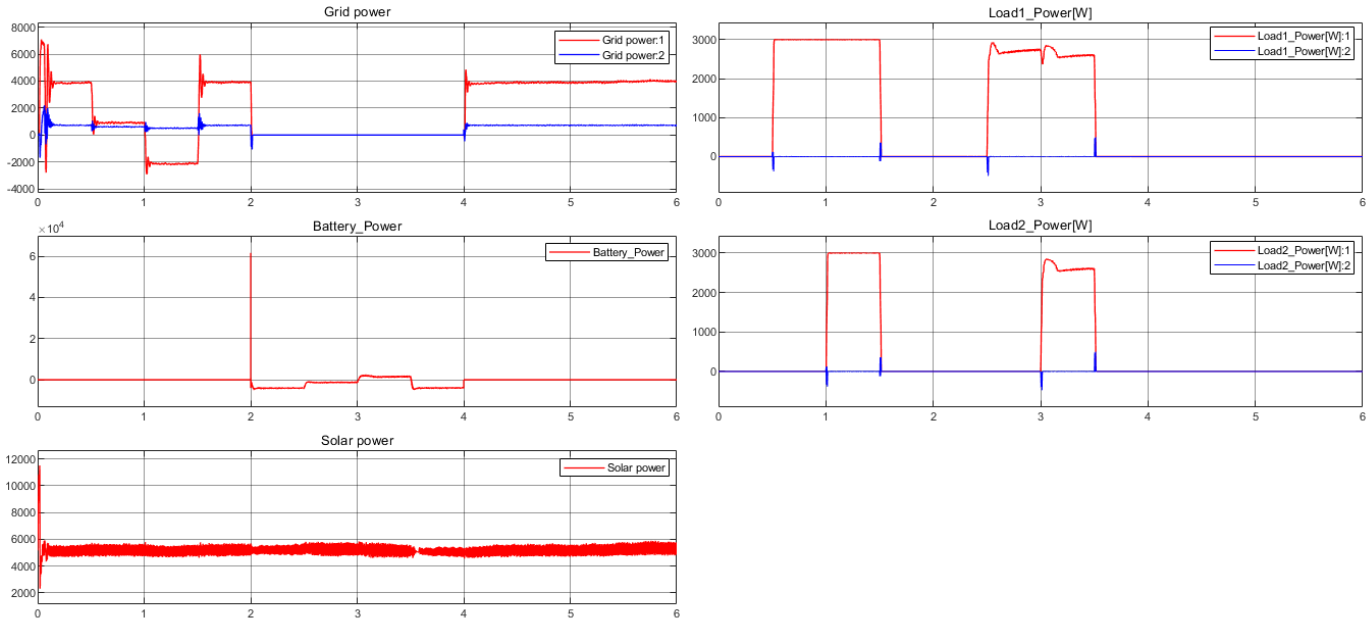

Figure 4.3: Power Outputs from the solar and grid and load consumptions.

When the grid is active, it powers the loads and may even recharge the battery.

When the grid goes offline (around 2 seconds), the battery and solar systems seamlessly take over.

Solar power provides a constant contribution, while the battery supplies additional power during high demand or when the grid is offline.

The transition between power sources is managed to ensure uninterrupted power supply to the loads.

4.3 Grid Monitoring

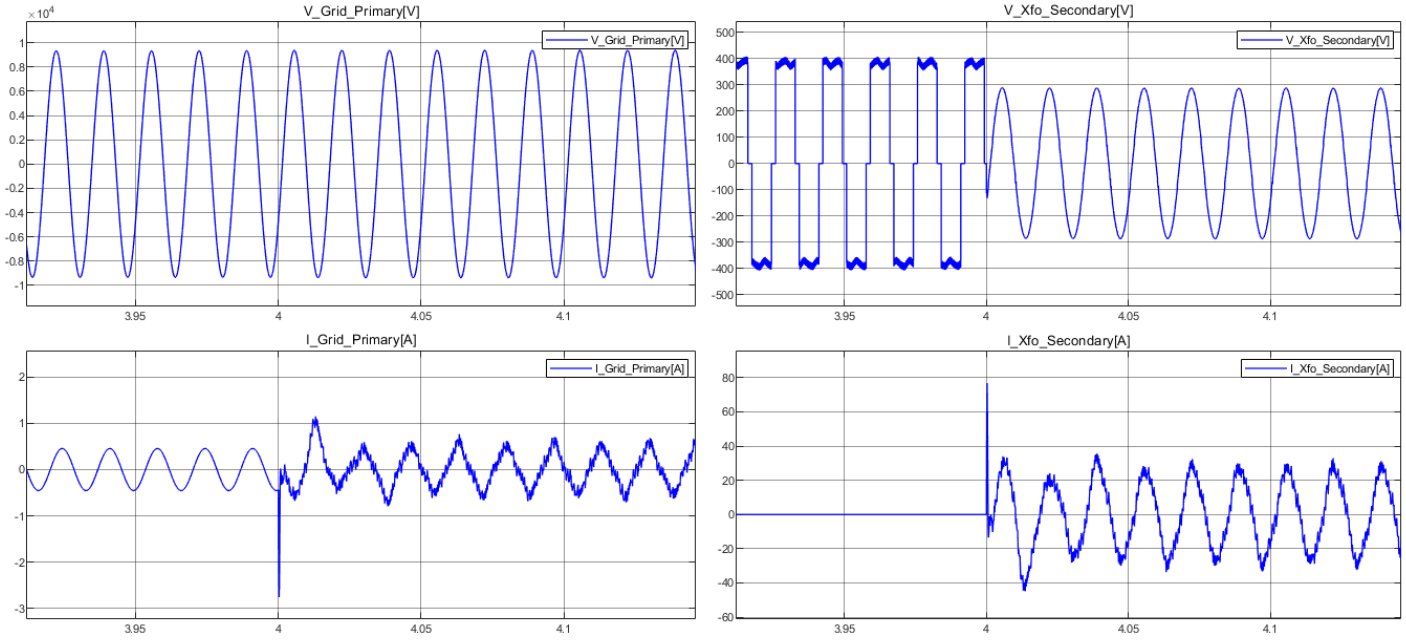

Figure 4.4: Grid Monitoring

The graphs demonstrate the interconnected nature of the primary and secondary sides in a grid system. Any disturbance on one side directly impacts the other, emphasizing the importance of stability and protection mechanisms in such systems.

1. V_Grid_Primary: The primary voltage remains sinusoidal until a disturbance occurs around 4 seconds.

2. V_Xto_Secondary: The secondary voltage mirrors the primary, with a similar disturbance around 4 seconds.

3. I_Grid_Primary: The primary current shows sinusoidal behavior with transients appearing after 4 seconds.

4. I_Xto_Secondary: The secondary current initially stable, exhibits disturbances corresponding to the primary side at 4 seconds.

4.4 prototype Implemented

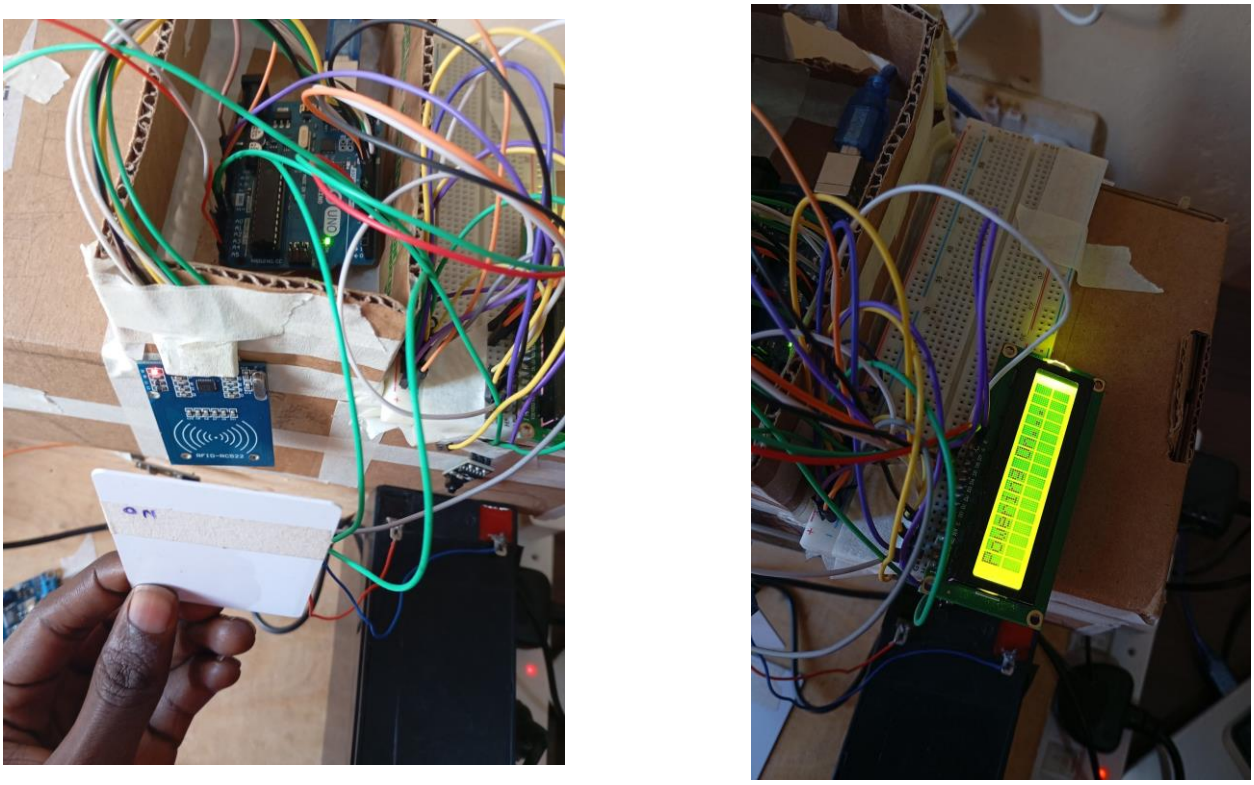

Figure 4.5: System Power ON

An Rfid tag is used to activate the charging system and the status is monitored through an LCD.

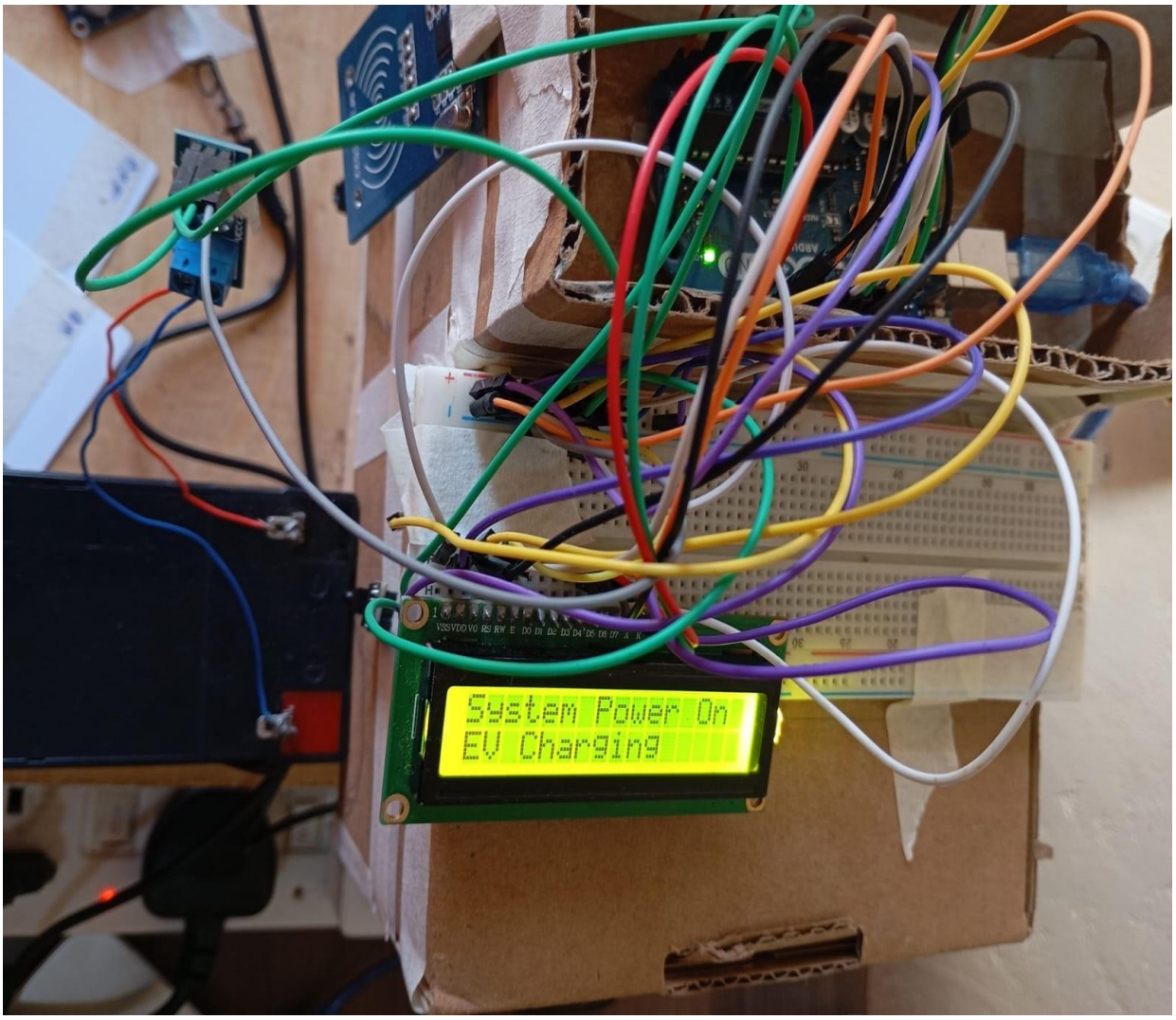

Figure 4.6: System Charging

On successful activation, the system acknowledges the charging request and begins charging the battery.

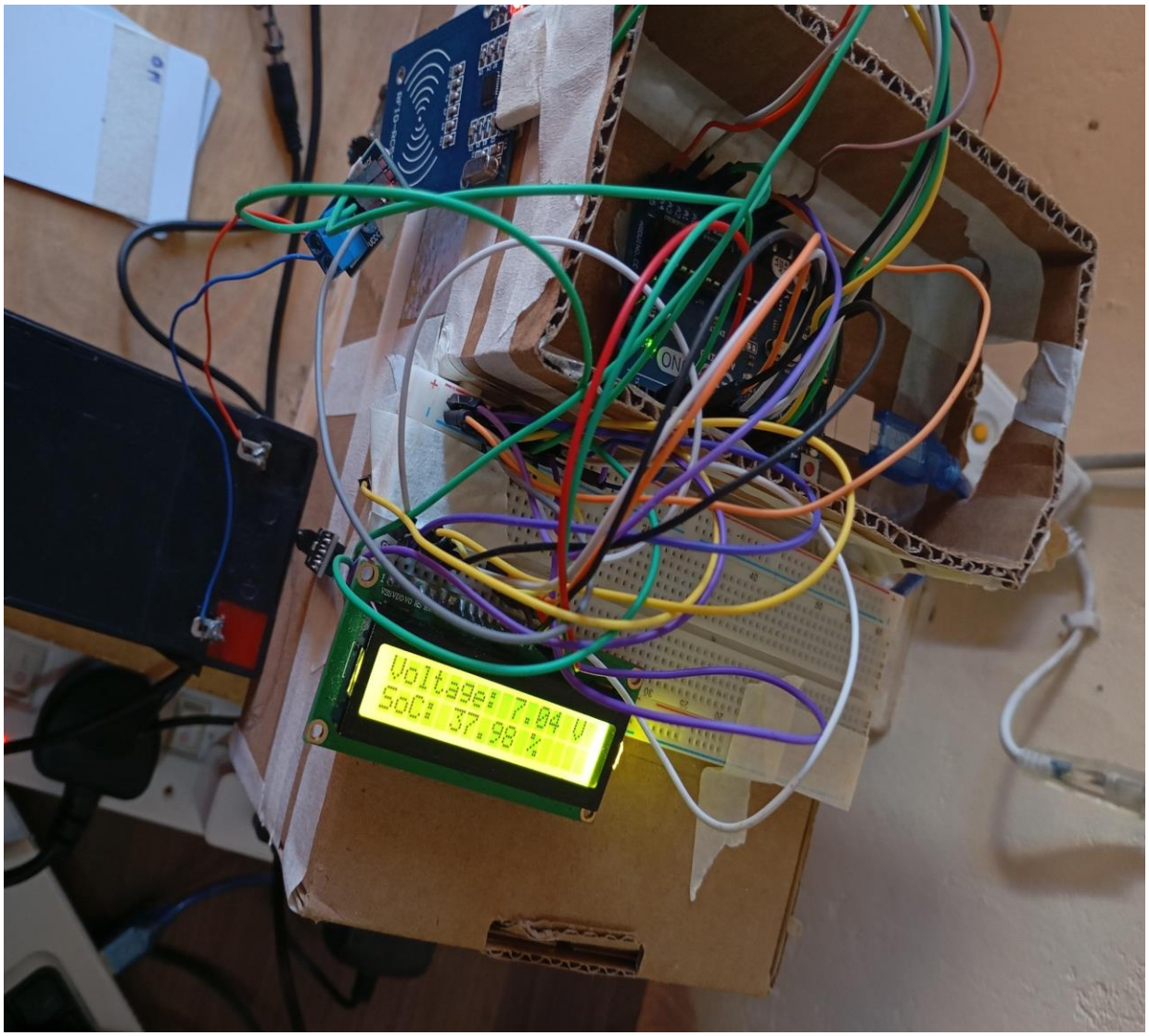

Figure 4.7: State of charge

The battery indication and level is shown for convenience and reliability

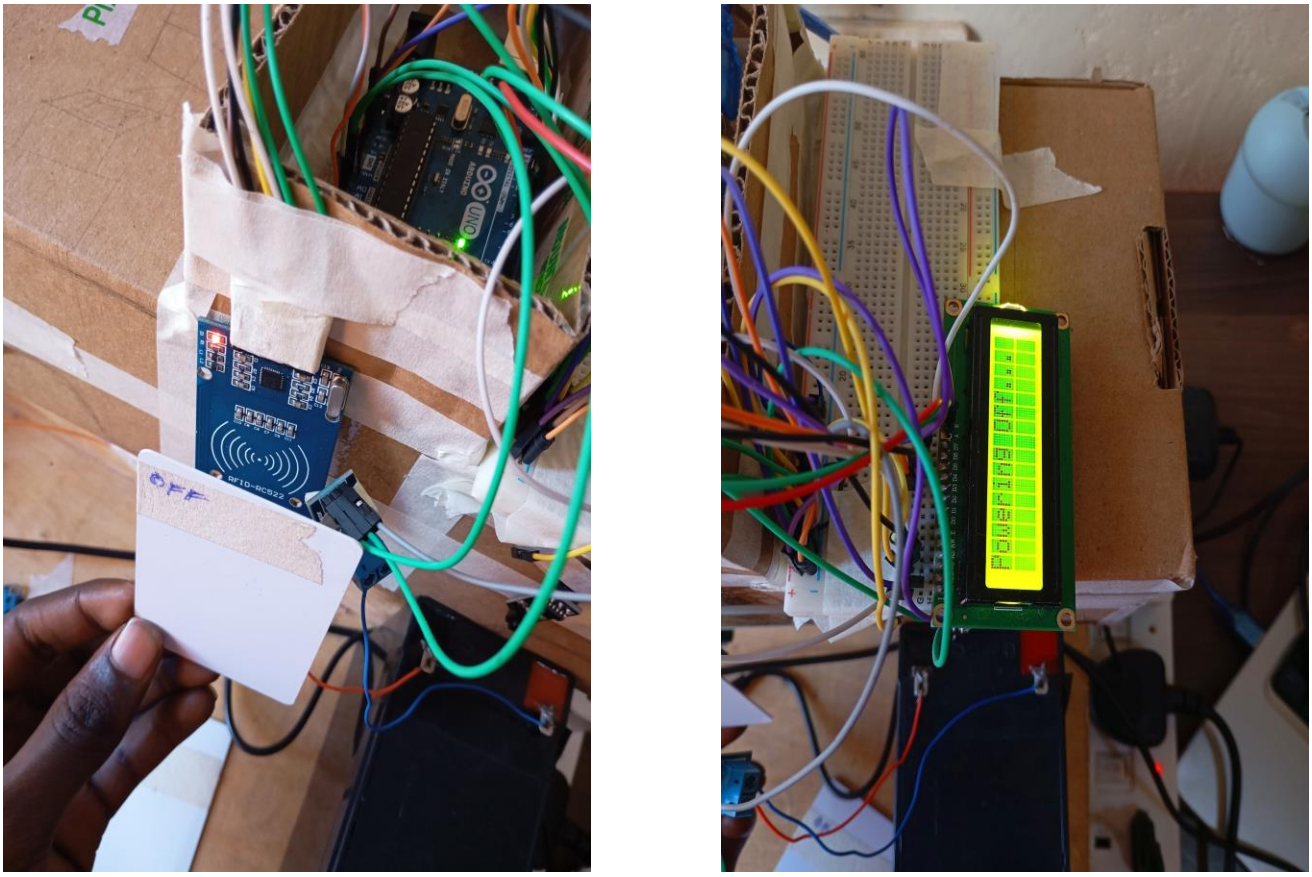

Figure 4.8: System Power off

On full charging, the user initiates the discharging request via an RFID TAG. Once the system recognizes the request, the power is disconnected.

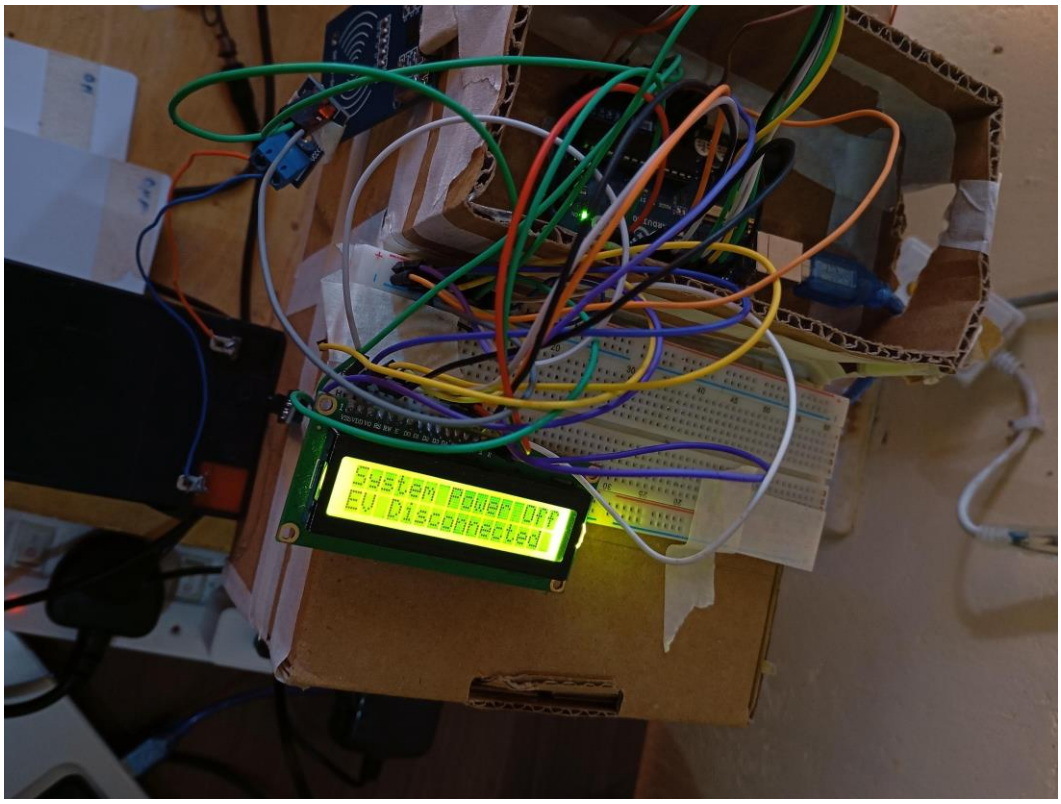

Figure 4.9: System Power Disconnected

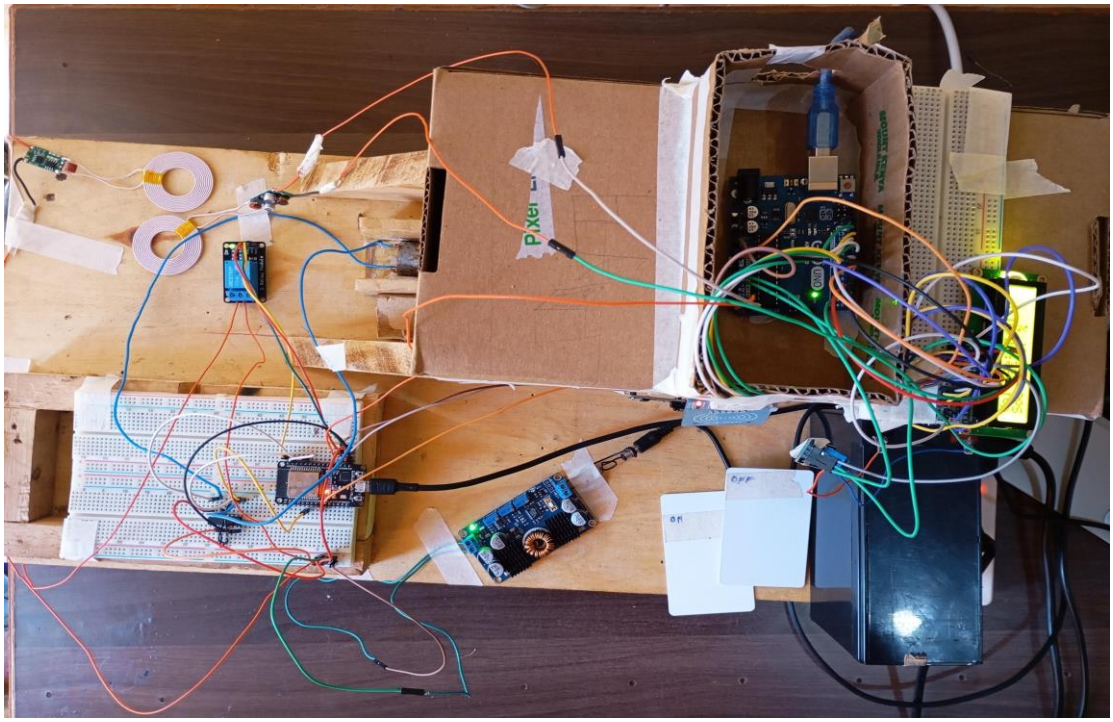

Figure 5.0: Full System

CHAPTER 5: CONCLUSIONS AND RECOMMENDATIONS

5.1 Conclusion

The Smart Electric Vehicle Wireless Charging System (SevWCS) provides an efficient, automated, and sustainable solution for EV charging. It reduces reliance on grid power through solar integration, ensures uninterrupted operation with an automatic changeover, and offers Realtime battery monitoring for a better user experience.

5.2 Recommendations

- Increase Solar Efficiency: Use advanced solar panels to enhance energy capture and reduce dependency on the grid.
- Test in Real Conditions: Conduct real-world trials to confirm the system's performance in various environments.
- Improve Charging Speed: Optimize the system to charge EV batteries faster without compromising efficiency.

References

[1] A. SOLUTIONS, "ALLEN ENERGY," ALLEN ENERGY, 1 12 2006. [Online]. Available: https://allenenergy.com/advances-in-wireless-charging/ [Accessed 8 12 2024].

[2] C. GROUP, "CIE-GROUP.COM," CIE GROUP, 6 DECEMBER 2019. [Online]. Available: https://cie-group.com/how-to-av/videos-and-blogs/what-is-wireless-inductive-charging. [Accessed 8 DECEMBER 2024].

[3] A. fuel, "Airfuel.org," [Online]. Available: https://cie-group.com/how-to-av/videos-and-blogs/what-is-wireless-inductive-charging. [Accessed 8 December 2024].

[4] "Techtarget.com," [Online]. Available: https://www.techtarget.com/whatis/definition/RF-wireless-charging-RF-energy-harvesting[Accessed 8 December 2024].

[5] L. Pearce Williams, "Faraday's discovery of electromagnetic induction. Contemporary Physics, 5(1),," p. 28–37., 1963.

[6] "inductive cahrging principles," 2010.

[7] W. B. Carlson, *Tesla: Inventor of the Electrical Age,* 2013.

[8] T. N., *Apparatus for Transmitting Electrical Energy, U.S. Patent 1,* pp. 19, 732, 1914.

[9] B. W. C., "The History of Power Transmission by Radio Waves," *IEEE Transaction on Microwave Theory Tech,* Vols. 32, no. 9, pp. 1230-42, 1984.

[10] K. Y. H. K. S. Y. L. M. L. L. J. M. Z. T. Cheon S, "Circuit-Model-Based Analysis of a Wireless Energy-Transfer," Vols. 58, No 7, p. 2906–2914, 2011.

[11] E. E. E. Brown W. C, "Beamed Microwave Power Transmission," *IEEE Trans Microw Theory Tech,* vol. 6, p. 1239–50, 1992.

[12] M. J. C. McSpadden J. O, "Space Solar Power Programs and Microwave Wireless Power Transmission Technology," *IEEE Microw mag,* vol. 40, no. 6, pp. 1239-50, 2002.

[13] B. J, "Space Applications of High-Power Microwaves,," *IEEE Trans Plasma Sci,* vol. 36, no. 3, pp. 569-581, 2008.

[14] edurev.init, April 2016. [Online]. Available: https://edurev.in/t/188034/Maxwell-s-Equations. [Accessed 8 December 2024].

[15] A. ENERGY, "ALLEN ENERGY," [Online]. Available: CHAPTER 1: INTRODUCTION. [Accessed 8 12 2024].

Appendices

Appendix 1: Budget

	A	B	C	D	E
1	**Item Number**	**Item Description**	**Quantity**	**Unit Price (KES)**	**Total Price (KES)**
2	Item 1	ESP32	1	1038	1038
3	Item 2	Arduino Uno	1	2000	2000
4	Item 3	LTC3780 Buck Converter	1	2250	2250
5	Item 4	RFID Reader/Detector	1	400	400
6	Item 5	Jumper Wires	1	300	300
7	Item 6	Panasonic 12V Battery	1	1500	1500
8	Item 7	AC DC Adapter	1	900	900
9	Item 8	Relay Module	1	150	150
10	Item 9	Wireless Charging Coils	1	1500	1500
11	Item 10	Breadboards	3	200	600
12	Item 11	LCD Display	1	250	250
13	Item 12	Voltage Sensor	1	200	200
14	Item 13	L293D Motor	1	300	300
15	Item 14	Brush DC Motor	1	1900	1900
16		Grand Total			13288

Appendix 2: codes used

Transmitter code

```
#include <Arduino.h>

#define IN1 22           // Motor IN1 pin
#define IN2 21           // Motor IN2 pin
#define ENA 32           // Motor Enable pin for speed control
#define RECEIVE_PIN 4    // Pin D4 to receive signal from Arduino
#define RELAY_PIN 23     // Relay control pin

int motorSpeed = 200;
bool prevTrackerSensorState = HIGH;

void setup() {
  pinMode(RECEIVE_PIN, INPUT);
  pinMode(IN1, OUTPUT);
  pinMode(IN2, OUTPUT);
  pinMode(ENA, OUTPUT);
  pinMode(RELAY_PIN, OUTPUT);

  // Initial states
  digitalWrite(IN1, LOW);
  digitalWrite(IN2, LOW);
  digitalWrite(RELAY_PIN, LOW);  // Relay off initially

  Serial.begin(9600);
  Serial.println("ESP32 Ready");
}

void loop() {
  int trackerSensorState = digitalRead(RECEIVE_PIN);

  Serial.print("Tracker Sensor State: ");
  Serial.println(trackerSensorState);

  // If an object is detected, activate relay and move motor clockwise
  if (trackerSensorState == HIGH && prevTrackerSensorState == LOW) {
    Serial.println("Object detected! Turning on relay and moving motor
clockwise.");

    // Turn on relay
    digitalWrite(RELAY_PIN, HIGH);

    // Motor moves clockwise
```

```
    analogWrite(ENA, motorSpeed);
    digitalWrite(IN1, HIGH);
    digitalWrite(IN2, LOW);
    delay(2000);

    // Stop motor
    digitalWrite(IN1, LOW);
    digitalWrite(IN2, LOW);
    delay(1000);
  }

  // If the object moves away, deactivate relay and move motor anticlockwise
  if (trackerSensorState == LOW && prevTrackerSensorState == HIGH) {
    Serial.println("Object moved away! Turning off relay and moving motor
anticlockwise.");

    // Turn off relay
    digitalWrite(RELAY_PIN, LOW);

    // Motor moves anticlockwise
    analogWrite(ENA, motorSpeed);
    digitalWrite(IN1, LOW);
    digitalWrite(IN2, HIGH);
    delay(2000);

    // Stop motor
    digitalWrite(IN1, LOW);
    digitalWrite(IN2, LOW);
    delay(1000);
  }

  // Update previous tracker sensor state for edge detection
  prevTrackerSensorState = trackerSensorState;
  delay(100);
}
```

Receiver code

```
#include <Arduino.h>
#include <MFRC522.h>
#include <SPI.h>
#include <LiquidCrystal.h>

// LCD pin assignments
const int rs = 7, en = 8, d4 = 5, d5 = 4, d6 = 3, d7 = 2;
LiquidCrystal lcd(rs, en, d4, d5, d6, d7);

// RFID settings
#define SS_PIN 10
#define RST_PIN 9
MFRC522 mfrc522(SS_PIN, RST_PIN);

// RFID UIDs
byte powerOnUID[4] = { 0xAE, 0xEE, 0x70, 0xD5 };  // UID for Power On
byte powerOffUID[4] = { 0x65, 0x9D, 0x40, 0xE6 }; // UID for Power Off

// Transmitter and induction pins
#define TRANSMIT_PIN A5         // Pin to control power on/off
#define INDUCTION_PIN A3        // Pin to detect charging status

// Battery sensor pin and voltage scaling factor
const int voltagePin = A0;               // Voltage sensor input
const float scalingFactor = 25.0 / 1023.0;  // Scale factor for MAX 25V sensor
on 10-bit ADC

// Battery parameters
const float maxVoltage = 12.0;
const float midVoltage = 8.0;
const float minVoltage = 4.0;

// Kalman filter parameters
const float Q = 0.001;
const float R = 0.01;
float P = 1.0;
float K;
float SoC = 1.0;
float estimatedVoltage = maxVoltage;

void setup() {
  Serial.begin(9600);
  lcd.begin(16, 2);
```

```
  // Initialize Transmitter pin
  pinMode(TRANSMIT_PIN, OUTPUT);
  digitalWrite(TRANSMIT_PIN, HIGH);  // Start with transmitter off

  // Initialize Induction pin
  pinMode(INDUCTION_PIN, INPUT);

  // Initialize RFID
  SPI.begin();
  mfrc522.PCD_Init();
}

void loop() {
  // **Section 1: Check Induction (Charging) Status**
  if (digitalRead(INDUCTION_PIN) == HIGH) {
    lcd.clear();
    lcd.print("System Power On");
    lcd.setCursor(0, 1);
    lcd.print("EV Charging");
    delay(2000);
  } else {
    lcd.clear();
    lcd.print("System Power Off");
    lcd.setCursor(0, 1);
    lcd.print("EV Disconnected");
    delay(2000);
  }

  // **Section 2: RFID Tag Reading for Power On/Off**
  if (mfrc522.PICC_IsNewCardPresent() && mfrc522.PICC_ReadCardSerial()) {
    if (checkUID(mfrc522.uid.uidByte, powerOnUID)) {
      if (digitalRead(INDUCTION_PIN) == LOW) {
        lcd.clear();
        lcd.print("Powering On...");
        digitalWrite(TRANSMIT_PIN, LOW);  // Activate the transmitter
        delay(2000);

        // Confirm power on
        if (digitalRead(INDUCTION_PIN) == HIGH) {
          lcd.clear();
          lcd.print("System Power On");
          lcd.setCursor(0, 1);
          lcd.print("EV Charging");
        } else {
          lcd.clear();
```

```
        lcd.print("Failed to Power On");
        delay(2000);
      }
    }
  } else if (checkUID(mfrc522.uid.uidByte, powerOffUID)) {
    if (digitalRead(INDUCTION_PIN) == HIGH) {
      lcd.clear();
      lcd.print("Powering Off...");
      digitalWrite(TRANSMIT_PIN, HIGH);  // Deactivate the transmitter
      delay(2000);

      // Confirm power off
      if (digitalRead(INDUCTION_PIN) == LOW) {
        lcd.clear();
        lcd.print("System Power Off");
        lcd.setCursor(0, 1);
        lcd.print("EV Disconnected");
      } else {
        lcd.clear();
        lcd.print("Failed to Power Off");
        delay(2000);
      }
    }
  }
  mfrc522.PICC_HaltA();
}

// **Section 3: Battery Voltage and SoC Calculation**
int sensorValue = analogRead(voltagePin);
float measuredVoltage = sensorValue * scalingFactor;
SoC = EKF_Update(measuredVoltage);

lcd.clear();
lcd.setCursor(0, 0);
lcd.print("Voltage: ");
lcd.print(measuredVoltage);
lcd.print(" V");

lcd.setCursor(0, 1);
lcd.print("SoC: ");
lcd.print(SoC * 100.0);  // Display SoC as percentage
lcd.print(" %");

delay(2000);  // Delay for readability
```

```
  // **Fault Detection**
  checkFaults(measuredVoltage);
}

// Function to check if UID matches the tag
bool checkUID(byte *readUID, byte *targetUID) {
  for (int i = 0; i < 4; i++) {
    if (readUID[i] != targetUID[i]) {
      return false;
    }
  }
  return true;
}

// Extended Kalman Filter (EKF) Update Function for SoC estimation
float EKF_Update(float measuredVoltage) {
  estimatedVoltage = minVoltage + (maxVoltage - minVoltage) * SoC;
  P = P + Q;

  K = P / (P + R);

  SoC = SoC + K * (measuredVoltage - estimatedVoltage);
  P = (1 - K) * P;

  SoC = calculateSoC(measuredVoltage);

  if (SoC > 1.0) SoC = 1.0;
  if (SoC < 0.0) SoC = 0.0;

  return SoC;
}

// Function to calculate SoC based on voltage readings
float calculateSoC(float voltage) {
  if (voltage >= maxVoltage) return 1.0;
  else if (voltage <= minVoltage) return 0.0;
  else return (voltage - minVoltage) / (maxVoltage - minVoltage);
}

// Function to check for overvoltage and undervoltage faults
void checkFaults(float voltage) {
  const float overVoltageLimit = 15.0;
  const float underVoltageLimit = 4.0;

  if (voltage > overVoltageLimit) {
```

```
    Serial.println("Fault: Overvoltage detected!");
  } else if (voltage < underVoltageLimit) {
    Serial.println("Fault: Undervoltage detected!");
  } else {
    Serial.println("Battery status: Normal");
  }
}
```